

## NEUROSCIENCE

# The long noncoding RNA FEDORA is a cell type– and sex-specific regulator of depression

Orna Issler<sup>1</sup>, Yentl Y. van der Zee<sup>1</sup>, Aarthi Ramakrishnan<sup>1</sup>, Sunhui Xia<sup>2</sup>, Alexander K. Zinsmaier<sup>2</sup>, Chunfeng Tan<sup>3</sup>, Wei Li<sup>3</sup>, Caleb J. Browne<sup>1</sup>, Deena M. Walker<sup>1</sup>, Marine Salery<sup>1</sup>, Angélica Torres-Berrio<sup>1</sup>, Rita Futamura<sup>1</sup>, Julia E. Duffy<sup>1</sup>, Benoit Labonte<sup>1</sup>, Matthew J. Girgenti<sup>4</sup>, Carol A. Tamminga<sup>3</sup>, Jeffrey L. Dupree<sup>5</sup>, Yan Dong<sup>2</sup>, James W. Murrrough<sup>1</sup>, Li Shen<sup>1</sup>, Eric J. Nestler<sup>1\*</sup>

Women suffer from depression at twice the rate of men, but the underlying molecular mechanisms are poorly understood. Here, we identify marked baseline sex differences in the expression of long noncoding RNAs (lncRNAs), a class of regulatory transcripts, in human postmortem brain tissue that are profoundly lost in depression. One such human lncRNA, RP11-298D21.1 (which we termed FEDORA), is enriched in oligodendrocytes and neurons and up-regulated in the prefrontal cortex (PFC) of depressed females only. We found that virally expressing FEDORA selectively either in neurons or in oligodendrocytes of PFC promoted depression-like behavioral abnormalities in female mice only, changes associated with cell type–specific regulation of synaptic properties, myelin thickness, and gene expression. We also found that blood FEDORA levels have diagnostic implications for depressed women and are associated with clinical response to ketamine. These findings demonstrate the important role played by lncRNAs, and FEDORA in particular, in shaping the sex-specific landscape of the brain and contributing to sex differences in depression.

## INTRODUCTION

Major depressive disorder (MDD) is a devastating psychiatric syndrome and among the leading causes of disability worldwide (1, 2). Available treatments, including antidepressant medications and psychotherapy, have limited response and remission rates, with more than half of patients remaining at least partly treatment resistant (3, 4). There are pronounced sex differences in MDD, as women are twice as likely to suffer from depression as men (1, 5). Moreover, women tend to have a different subset of symptoms, which are often more severe (5), and respond differentially to mechanistically divergent antidepressants compared to men (6). These sex differences are partially attributable to a higher sensitivity of women's stress responses (7) and fluctuations in ovarian hormones (8, 9). However, these mechanisms do not explain why only a subset of women develop depression (10). Shedding light on the molecular processes associated with sex differences in MDD could promote the development of sex-specific diagnostic and treatment approaches.

Epigenetic processes have been proposed as important mediators of gene environment interactions that lead to MDD (3, 11). One important arm of epigenetic regulation is long noncoding RNAs (lncRNAs), a class of transcripts longer than 200 nucleotides with no apparent protein-coding role (12, 13). Notably, about 40% of lncRNAs are brain specific, with many of these molecules arising in primate evolution and coinciding with an increase in brain size (14). lncRNAs have similar structural features to mRNAs; however, they are often expressed at low levels and exhibit notable region- and

cell type–specific patterns (15). Functionally, lncRNAs can act as scaffolds, guides, or decoys, leading to changes in the expression of protein-coding genes (PCGs) (16). We and others reported regulation of specific lncRNAs in postmortem brain tissue of MDD patients (17, 18) and rodent stress models (19, 20). However, a global analysis of baseline sex differences in lncRNA expression levels in the brain and how this pattern is altered in MDD has not yet been performed.

The present study reports that robust baseline sex differences in lncRNA expression patterns in several limbic brain regions examined postmortem from healthy control (HC) subjects that are markedly lost in MDD. We highlight one such human-specific lncRNA, RP11-298D21.1, which we named FEDORA, that is expressed to a lower degree in female HCs compared to males across several brain regions examined. This pattern is reversed in MDD: FEDORA is up-regulated in females with MDD compared to HCs, with no change seen in males. FEDORA expression in the brain predominates in oligodendrocytes and, to a lesser extent, in neurons. We hypothesize that this lncRNA is a key sex-specific and cell type–specific regulator of mood. To test this hypothesis, we virally expressed FEDORA in the prefrontal cortex (PFC) selectively in either neurons or oligodendrocytes in mice of both sexes, followed by comprehensive phenotyping. We report that, while FEDORA expression in both cell types promotes depression-like behavior in female mice only, this effect is mediated by opposing transcriptional changes in neurons compared to oligodendrocytes. We also show that expression of FEDORA in mouse PFC neurons alters their electrophysiological activity, while expression of FEDORA in oligodendrocytes regulates myelin thickness. Last, we show that FEDORA levels in circulating blood are up-regulated only in females with MDD, with normalization of FEDORA expression correlating with the degree of clinical improvement seen in response to the rapidly acting antidepressant ketamine. Together, this study highlights the importance of lncRNAs in the brain, both in maintaining baseline sex differences

Copyright © 2022  
The Authors, some  
rights reserved;  
exclusive licensee  
American Association  
for the Advancement  
of Science. No claim to  
original U.S. Government  
Works. Distributed  
under a Creative  
Commons Attribution  
NonCommercial  
License 4.0 (CC BY-NC).

<sup>1</sup>Nash Family Department of Neuroscience, Friedman Brain Institute, Icahn School of Medicine at Mount Sinai, New York, NY, USA. <sup>2</sup>Department of Neuroscience, University of Pittsburgh, Pittsburgh, PA, USA. <sup>3</sup>Department of Psychiatry, UT Southwestern, Dallas, TX, USA. <sup>4</sup>Department of Anatomy and Neurobiology, Virginia Commonwealth University, Richmond, VA, USA. <sup>5</sup>Department of Psychiatry, Yale University School of Medicine, New Haven, CT, USA.

\*Corresponding author. Email: eric.nestler@mssm.edu

and MDD pathophysiology, and supports the view that FEDORA serves as a key regulator of these processes.

## RESULTS

### Abnormal expression of FEDORA in female MDD

In a recent study, we reported robust sex- and brain site-specific regulation of lncRNAs in postmortem brain tissue of subjects with MDD compared to HCs (17). Using this rich dataset, the present work focused on lncRNAs that demonstrate baseline sex differences, that is, are differentially expressed between male versus female HC subjects (fold change > 30% and nominal  $P < 0.05$ ). Comparing MDD with HC subjects, we noted a marked loss of these baseline sex differences in lncRNA expression. In the ventral medial PFC (vmPFC), we identified 762 lncRNAs with baseline sex differences, with 65.9% of these lncRNAs losing their baseline pattern of sex-specific expression in MDD subjects (Fig. 1A and table S5). We found a similar phenomenon in each of the five other brain regions examined, which included dorsolateral PFC (dlPFC), orbitofrontal cortex (OFC), ventral subiculum (vSUB), anterior insula (aINS), and nucleus accumbens (NAc) (fig. S1, A to E, and table S5), and this effect was more pronounced when compared to the same analysis performed on PCGs (e.g., vmPFC = 45.1%; Fig. 1B and table S6). We observed two common patterns of regulation: The first was lncRNAs exhibiting lower expression in female versus male HCs that are up-regulated in female patients with MDD but down-regulated (or not affected) in male patients with MDD (Fig. 1C), and the second was lncRNAs exhibiting higher expression in female versus male HCs that are down-regulated in female patients with MDD but up-regulated (or not affected) in male patients with MDD (Fig. 1D). This phenomenon was replicated in an independent, previously published cohort (21) of postmortem brains of depressed and control subjects of both sexes (fig. S2). These findings suggest that lncRNAs play a key role in regulating sex differences in the brain and that this pattern is corrupted by MDD.

We hypothesize that lncRNAs that lose their baseline sex differences in MDD may have a critical mechanistic role in the molecular processes leading to sex differences in the pathophysiology of MDD. To identify these specific candidates, we probed the list of lncRNAs that demonstrated baseline sex differences (422 lncRNAs on average across brain regions) and filtered for those that broadly lost their baseline sex differences in MDD (73 lncRNAs in four or more of the brain regions analyzed). Next, we selected for lncRNAs that show a significant correlation in their expression levels to at least one PCG within our datasets ( $R > 0.587$  or  $R < -0.595$ ; 19 lncRNAs), are consistently expressed in the brain [count per million (CPM) > 1; 15 lncRNAs] and are differentially expressed in MDD in either sex (fold change > 30% and nominal  $P < 0.05$ ). This analysis revealed an antisense lncRNA called RP11-298D21.1 or AC009063.2 (Fig. 2A). This lncRNA displays a baseline sex difference as it is expressed at lower levels in female versus male HCs and is up-regulated in females with MDD compared to HCs across all brain regions studied, with no abnormal expression seen in males with MDD (Fig. 2B). On the basis of this expression pattern, we named the lncRNA Female DepressiOn lncRNA (FEDORA). We validated these results for the vmPFC using a combined cohort including the same samples used for RNA sequencing (RNA-seq) and an additional cohort (see table S1 for cohort demographics). We noted that FEDORA is up-regulated in females with MDD compared to HCs [two-way analysis of variance (ANOVA),  $F$  interaction<sub>1,75</sub> = 5.556,  $P = 0.021$ , post hoc Fisher least significant difference (LSD), HC (female) versus MDD (female)  $t_{75} = 1.946$ ,  $P = 0.0409$ ]. FEDORA is also expressed at higher levels in male compared to female HCs in this larger cohort, consistent with a reversal of this baseline sex difference in MDD [post hoc Fisher LSD HC (female) versus HC (male)  $t_{75} = 2.269$ ,  $P = 0.0261$ ; Fig. 2C]. Notably, there were no correlations between FEDORA levels and demographic features of these cohorts (fig. S3E).

FEDORA is a human-specific antisense RNA of *Cdh13*, which encodes cadherin-13 (22). FEDORA is enriched in the brain (fig. S3A) (23), where it is predominantly expressed in oligodendrocytes and

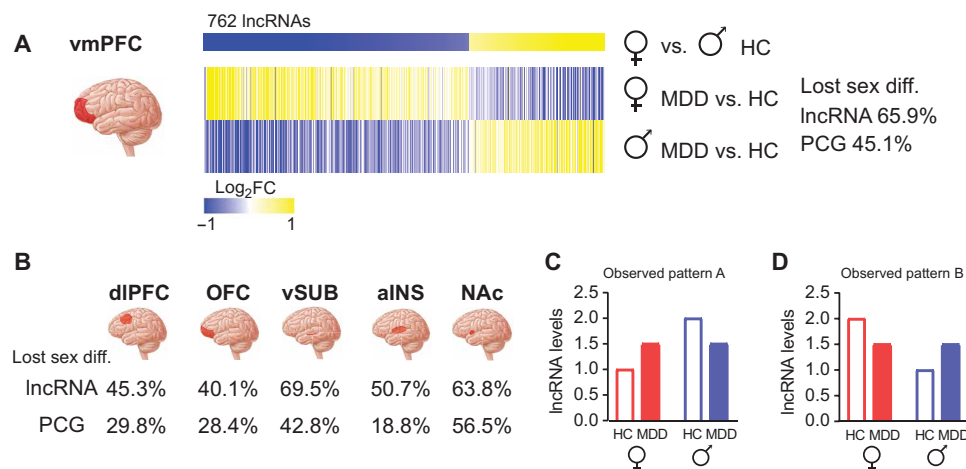


**Fig. 1. Baseline sex differences in lncRNA expression are lost in MDD.** (A) Heatmaps demonstrating that lncRNAs in vmPFC that exhibit baseline sex differences between female and male HCs (differential expression fold change > 30% and nominal  $P < 0.05$ ) are robustly oppositely altered in females versus males with MDD compared to HCs. Yellow represents up-regulation and blue down-regulation between log<sub>2</sub>fold change =  $\pm 1$ . (B) Baseline sex differences are also lost in MDD in the dlPFC, OFC, vSUB, aINS, and NAc. The percentage of lncRNAs and PCGs that lose this baseline sex difference in MDD is indicated. (C and D) Bar graphs representing the most commonly observed patterns of regulation of lncRNAs that lose baseline sex differences in MDD. RNA-seq dataset is from (29).  $n = 9$  to 13 per group.

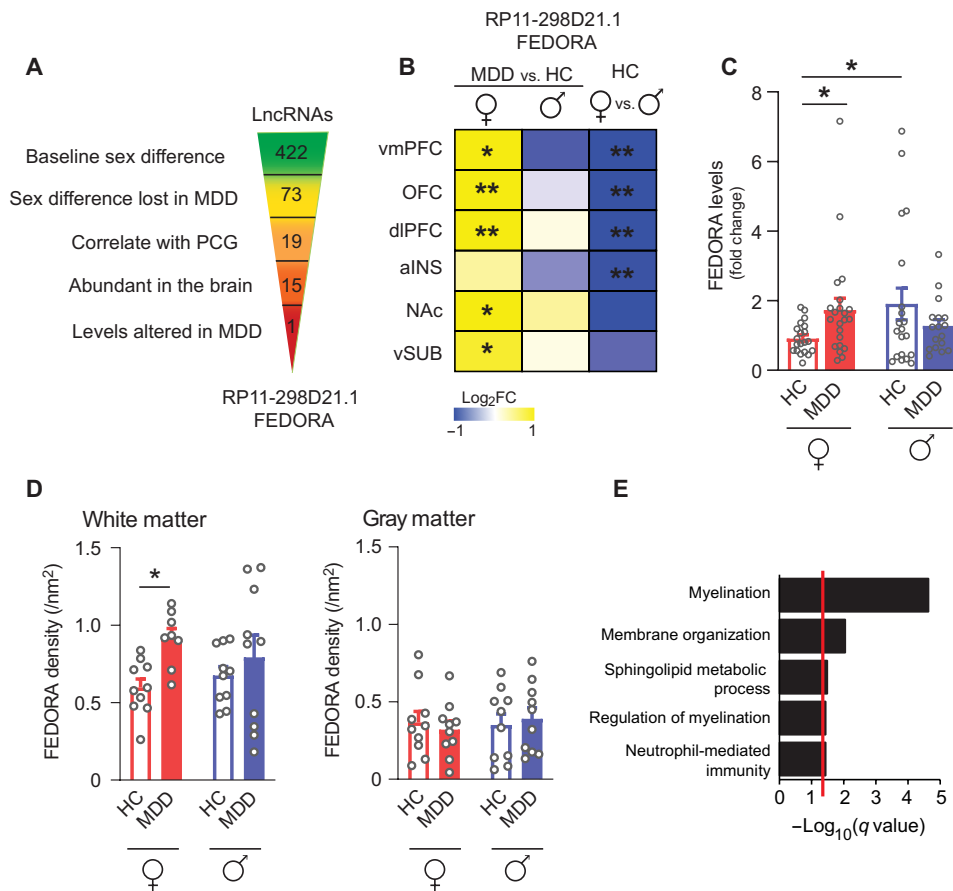


**Fig. 2. FEDORA lncRNA, a human oligodendrocyte- and neuronal-enriched transcript, is up-regulated in female MDD.** (A) Schematic representation of lncRNA filtering process identifying RP11-298D21.1 (FEDORA). lncRNAs with baseline sex differences (averaged across brain regions) were refined to those that (i) lost this baseline difference in MDD in at least four brain regions, (ii) exhibit significant correlation with at least one PCG within our female postmortem brain dataset, (iii) are abundant in the human brain (CMP > 1), and (iv) are differentially expressed in MDD (FC > 30% and nominal  $P < 0.05$ ). (B) Heatmaps representing RNA-seq results of the differential expression of FEDORA in female, but not male, MDD compared to HCs, as well as a baseline sex difference in HCs between female and male. Nominal  $*P < 0.05$  and  $**P < 0.01$ .  $n = 9$  to 13 per group. (C) Bar graph of qPCR validation results from a combined cohort of the samples used for RNA-seq and additional samples showing higher levels of FEDORA in males compared to females in the HCs and up-regulation of FEDORA in females with MDD, with no effect of MDD seen in males. Fisher LSD post hoc,  $*P < 0.05$ .  $n = 17$  to 21 per group. Bars represent means  $\pm$  SEM, and dots represent individual data points. (D) Bar graph of quantification of FISH for FEDORA in rostral anterior cingulate cortex (rACC) of an independent cohort of human brain postmortem samples. The data show that FEDORA is expressed at higher levels in white matter than in gray matter and is up-regulated in females with MDD compared to HCs. Fisher LSD post hoc,  $*P < 0.05$ .  $n = 10$  per group. (E) Bar graph representing top enriched gene ontology (GO) terms of PCGs ( $n = 360$ ) whose expression levels are significantly correlated with FEDORA in the female brain. The red line represents FDR-corrected  $q = 0.05$ .

neurons to a lesser extent (fig. S3B) (24). We validated the regulation of FEDORA in MDD and its cell type-specific expression pattern using in situ hybridization in the rostral anterior cingulate cortex (rACC) from an independent cohort of MDD and HC subjects of both sexes. We found that FEDORA colocalizes with markers for both neurons and oligodendrocytes (fig. S3, C and D), with higher levels of FEDORA in white matter than in gray matter (two-way ANOVA in control subject,  $F$  main effect tissue<sub>1,36</sub> = 9.621,  $P = 0.0037$ ; Fig. 2D). Within white matter, we found higher levels of FEDORA in females with MDD compared to controls, an effect not seen in males (two-way ANOVA,  $F$  main effect group<sub>1,34</sub> = 5.733,  $P = 0.0223$ ; Fig. 2D). Gene ontology analysis performed on the list of 360 PCGs that significantly correlate with FEDORA levels in the female brain within our dataset implicated myelination-related processes (Fig. 2E), supporting a potential role for FEDORA in oligodendrocyte function.

### Behavioral effects of FEDORA expression in mouse mPFC

To determine whether FEDORA has a causal sex- and cell type-specific role in promoting MDD, we “humanized” mice for this transcript by virally expressing it selectively in either neurons or oligodendrocytes. First, we developed a neuron-specific tool to express FEDORA in mouse mPFC along with a green fluorescent protein (GFP) reporter (Neuro-FEDORA), or GFP only as control (Neuro-GFP), using herpes simplex virus (HSV), which is highly neurotropic (Fig. 3A). We validated that this tool promotes FEDORA expression using quantitative polymerase chain reaction (qPCR; fig. S4A) and that the expression of FEDORA is neuron specific by colocalizing Neuro-GFP with neuronal, but not with oligodendrocyte or astrocytic, markers using immunohistochemistry (fig. S4B). There were equivalent glial fibrillary acidic protein (GFAP) signals, a marker of reactive astrocytes, in the mPFC near the needle track in mice injected with Neuro-GFP, Neuro-FEDORA, or vehicle

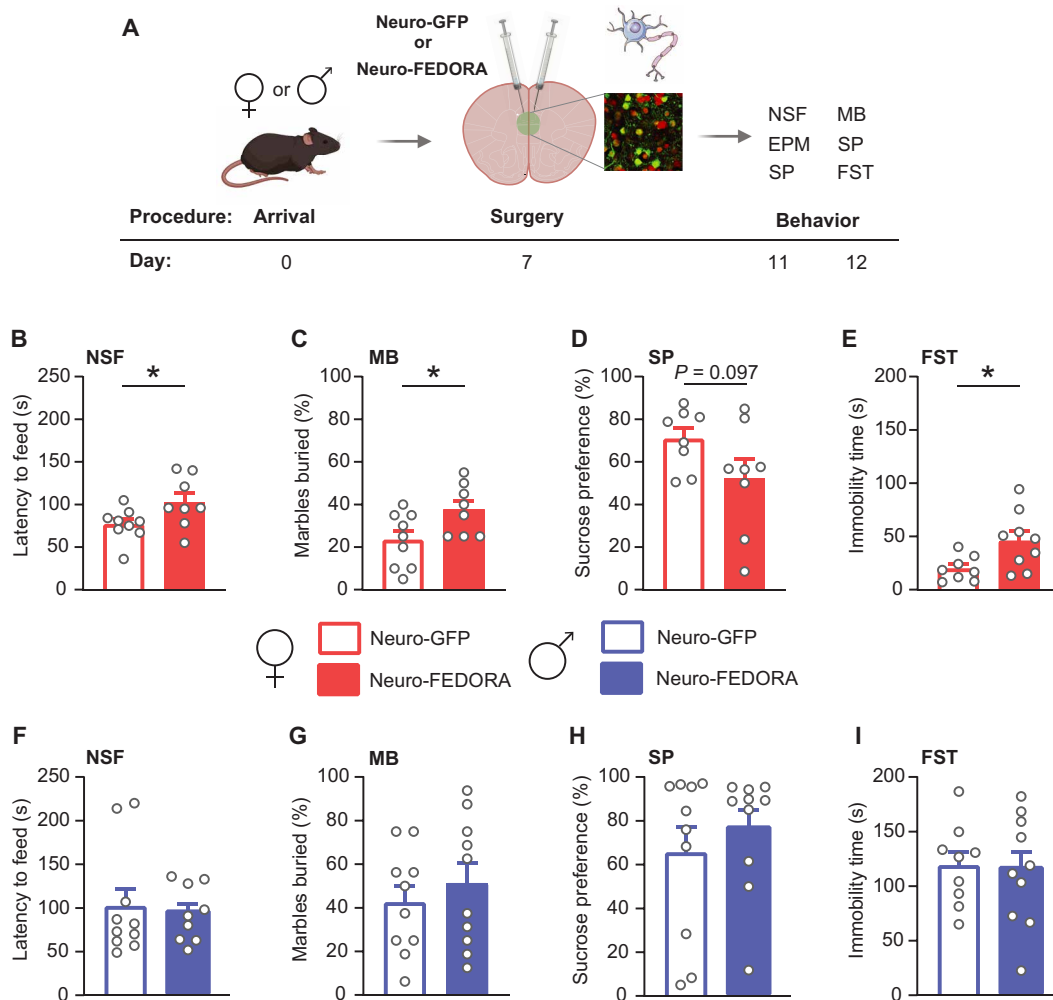


**Fig. 3. Expression of FEDORA in mouse mPFC neurons promotes anxiety- and depression-related behavioral abnormalities in females only.** (A) Schematic representation and timeline of the experimental design. NSF, novelty-suppressed feeding; EMP, elevated plus maze; SP, sucrose preference; MB, marble burying; FST, forced swim test. (B to E) In females, Neuro-FEDORA promotes increased latency to feed in the novelty-suppressed feeding test (B), increased number of marbles buried (C), trend for decreased sucrose preference (D), and longer immobility time in the forced swim test (E). (F to I) No difference in any test was observed in male mice.  $n = 8$  to 10/group, Student's  $t$  test,  $*P < 0.05$ . Bars represent means  $\pm$  SEM, and dots represent individual data points.

[phosphate-buffered saline (PBS)] (fig. S4E) and similar weight changes in the same mice when compared before and after surgery (fig. S5H). In addition, we found no detectable Fluoro-Jade staining, a widely used and sensitive marker for necrosis, in brain slices of mice injected intra-PFC with either Neuro-GFP, Neuro-FEDORA, or vehicle. Together, these findings replicate numerous previous studies that document the lack of detectable toxicity with the use of our helper virus-free HSV vectors (25).

Next, we infected the mPFC of female and male adult mice with Neuro-FEDORA or Neuro-GFP and subsequently performed a battery of tests to measure anxiety- and depression-related behaviors. In female mice, Neuro-FEDORA compared to Neuro-GFP led to a longer latency to feed in the novelty-suppressed feeding test (Student's  $t$  test,  $t_{15} = 2.180$ ,  $P = 0.0456$ ; Fig. 3B), more marbles buried in the marble burying test (Student's  $t$  test,  $t_{15} = 2.351$ ,  $P = 0.0326$ ; Fig. 3C), a trend for lower sucrose preference (Student's  $t$  test,  $t_{14} = 1.779$ ,  $P = 0.0970$ ; Fig. 3D), an increase in immobility time in the forced swim test (Student's  $t$  test,  $t_{15} = 2.537$ ,  $P = 0.0228$ ; Fig. 3E), no difference in

time spent in the open arms of the elevated plus maze (fig. S5A), and a trend for shorter latency to immobility in a tail suspension test (Student's  $t$  test,  $t_{11} = 1.890$ ,  $P = 0.0854$ ; fig. S5G) with no differences in total time spent immobile (fig. S5F). There was no effect of Neuro-FEDORA on female mouse locomotion as reflected in the total distance traveled in the elevated plus maze (fig. S5B) or an open field test (fig. S5E), a further indication (along with normal weights as noted above) of the general health of virus-treated animals. A separate cohort of female mice was tested following the same viral treatments and exposure to 3 days of chronic variable stress (CVS) performed as described previously (26). There was no strong additive effect of stress in the behavioral end points analyzed (fig. S5, I to L). In male mice, we did not observe any differences across behavioral tests (Fig. 3, F to I, and fig. S5, C and D), supporting a female-specific increase in anxiety- and depression-like behaviors induced by neuronal expression of FEDORA in the mPFC, which mirrors the human female-specific increase in FEDORA levels in MDD.

We next expressed FEDORA in mPFC oligodendrocytes using a modified adeno-associated virus (AAV) with a truncated version of human myelin-associated glycoprotein (MAG) promoter to guide cell type specificity. We generated AAVs expressing FEDORA along with a GFP reporter (Oligo-FEDORA) or GFP only as control

(Oligo-GFP) (Fig. 4A), validated that this tool promotes FEDORA expression (fig. S4C), and confirmed that this expression predominates in oligodendrocytes (fig. S4D). We probed the sex-specific effect of Oligo-FEDORA in the mPFC of mice on anxiety- and depression-like behavioral phenotypes. We found that females treated with

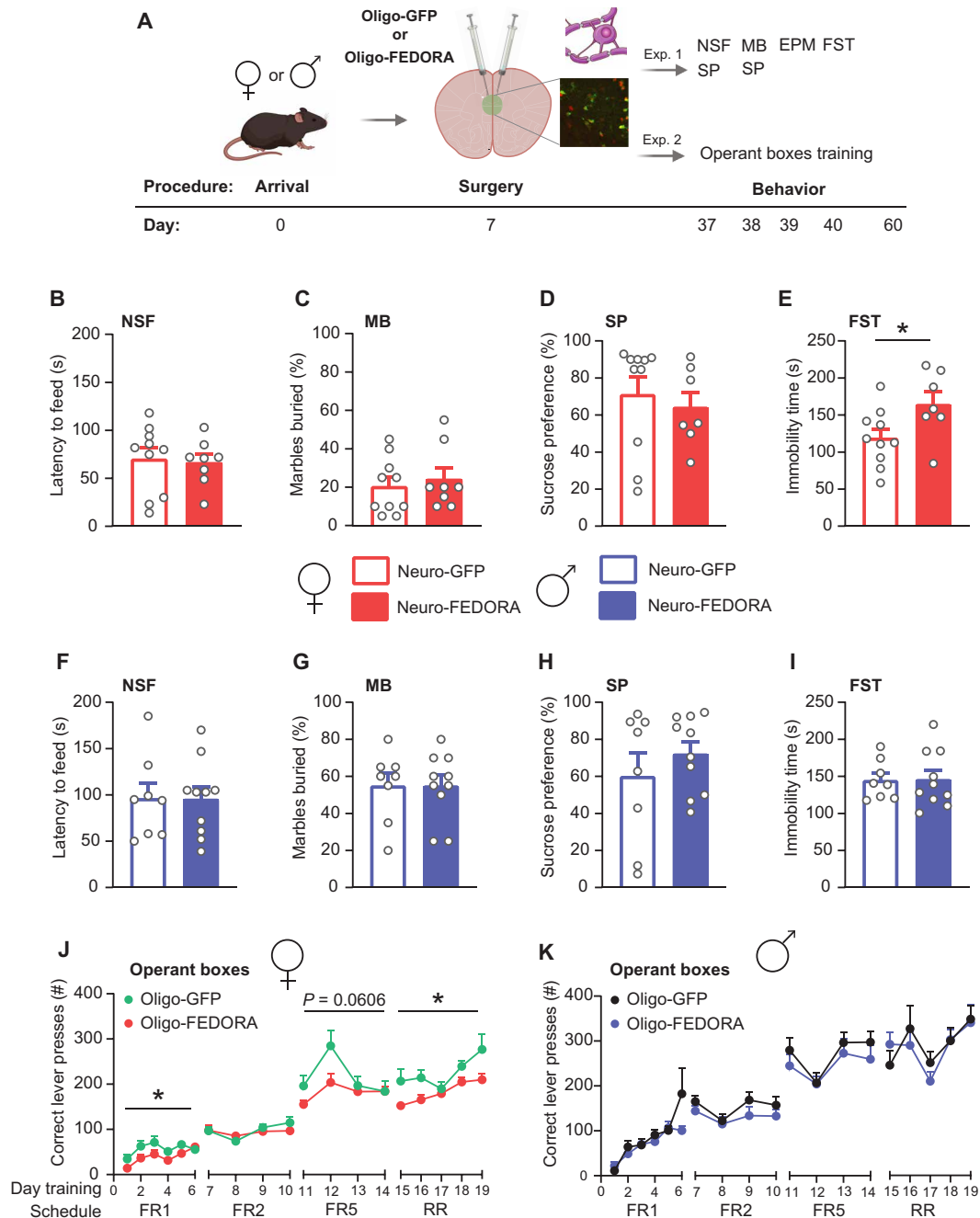


**Fig. 4. Expression of FEDORA in mouse mPFC oligodendrocytes promotes passive coping and attenuates reward learning in females only.** (A) Schematic representation and timeline of the experimental design. (B to E) Bar graphs depicting that, in females, Oligo-FEDORA compared to Oligo-GFP does not alter behavior in the novelty-suppressed feeding (B), marble burying (C), and sucrose preference (D) tests but leads to increased immobility time in the forced swim test (E). (F to I) No difference in any test was observed in male mice.  $n = 8$  to 10 group, Student's  $t$  test,  $*P < 0.05$ . Bars represent means  $\pm$  SEM, and dots represent individual data points. (J and K) Graph representing results on operant box task of training to lever press for liquid saccharin reward. Oligo-FEDORA female mice exhibited fewer correct lever presses than the Oligo-GFP group in the FR1 schedule and RR schedule, but not in the FR2 and FR5 schedule (J). For male mice, there were no differences between the groups (K).  $n = 10$  to 12 per group, two-way ANOVA repeated measure; main effect for virus,  $*P < 0.05$ . Circles represent means  $\pm$  SEM.

Oligo-FEDORA, compared to Oligo-GFP, showed increased immobility time in the forced swim test (Student's *t* test,  $t_{15} = 2.248$ ,  $P = 0.0401$ ; Fig. 4E), with no effect seen in the other tests in females including general locomotion (Fig. 4, B to D, and fig. S6, A, B, and E). Oligo-FEDORA had no effect in males across all tests used (Fig. 4, F to I, and fig. S6, C and D).

To further explore the oligodendrocyte role of FEDORA in mice in regulating motivation- and reward-related behaviors, we infused Oligo-FEDORA or Oligo-GFP into the mPFC of an additional cohort of mice and trained them on an operant reinforcement task to press a lever to receive a liquid saccharin reward. Oligo-FEDORA treatment did not affect sucrose preference (Fig. 4D), suggesting that this manipulation does not affect the hedonic value of this reward. However, Oligo-FEDORA female mice demonstrated a lower number of correct lever presses compared to Oligo-GFP mice during the acquisition of responding for the saccharin reward on a fixed ratio 1 (FR1; one response = one reward) schedule of reinforcement (repeated measures two-way ANOVA,  $F_{virus_{1,20}} = 4.837$ ,  $P = 0.0398$ ; Fig. 4J). Oligo-FEDORA mice reached similar levels of responding by the end of FR1 acquisition and increasing the motivational demands of the task by increasing the schedule of reinforcement to FR2 or FR5 did not reveal a significant difference between the groups (Fig. 4J). However, switching to a more ambiguous random ratio 5 (RR5) schedule of reinforcement, wherein each response has a 20% probability of saccharin delivery (five responses per reward, on average), again revealed a deficit in performance in the Oligo-FEDORA female mice

(repeated measures two-way ANOVA,  $F_{virus_{1,20}} = 6.080$ ,  $P = 0.0228$ ; Fig. 4J). There was no effect for Oligo-FEDORA on the performance of male mice in any of the reinforcement schedules (Fig. 4K). Together, these results indicate that FEDORA expression in mPFC oligodendrocytes impairs reward learning and performance in females.

### Effects of FEDORA expression on neuronal and oligodendrocyte function

To explore how neuronal FEDORA mediates its female-specific prodepressive effects, we performed slice electrophysiological recordings from mPFC pyramidal neurons of mice of both sexes infected with either Neuro-FEDORA or Neuro-GFP as control. We found that neuronal FEDORA expression increased spontaneous excitatory postsynaptic current (sEPSC) amplitude (Student's *t* test,  $t_{13} = 2.281$ ,  $P = 0.0401$ ; Fig. 5, A and B) and frequency (Student's *t* test,  $t_{13} = 2.137$ ,  $P = 0.0522$ ; Fig. 5, A and C) in female, but not male, mice (Fig. 5, F to H). Moreover, we found that Neuro-FEDORA compared to Neuro-GFP decreased the excitability of mPFC pyramidal neurons upon current injection in both female (two-way ANOVA,  $F_{virus_{1,117}} = 35.82$ ,  $P < 0.0001$ ; Fig. 5, D and E) and male (two-way ANOVA,  $F_{virus_{1,108}} = 42.25$ ,  $P < 0.0001$ ; Fig. 5, I and J) mice. We have previously reported no difference between mPFC neuronal properties in Neuro-GFP versus vehicle mice, further supporting the lack of toxicity of our HSV vectors (17). Together, these results demonstrate both sex-specific and global effects of FEDORA expression on pyramidal neuron physiology in mPFC.

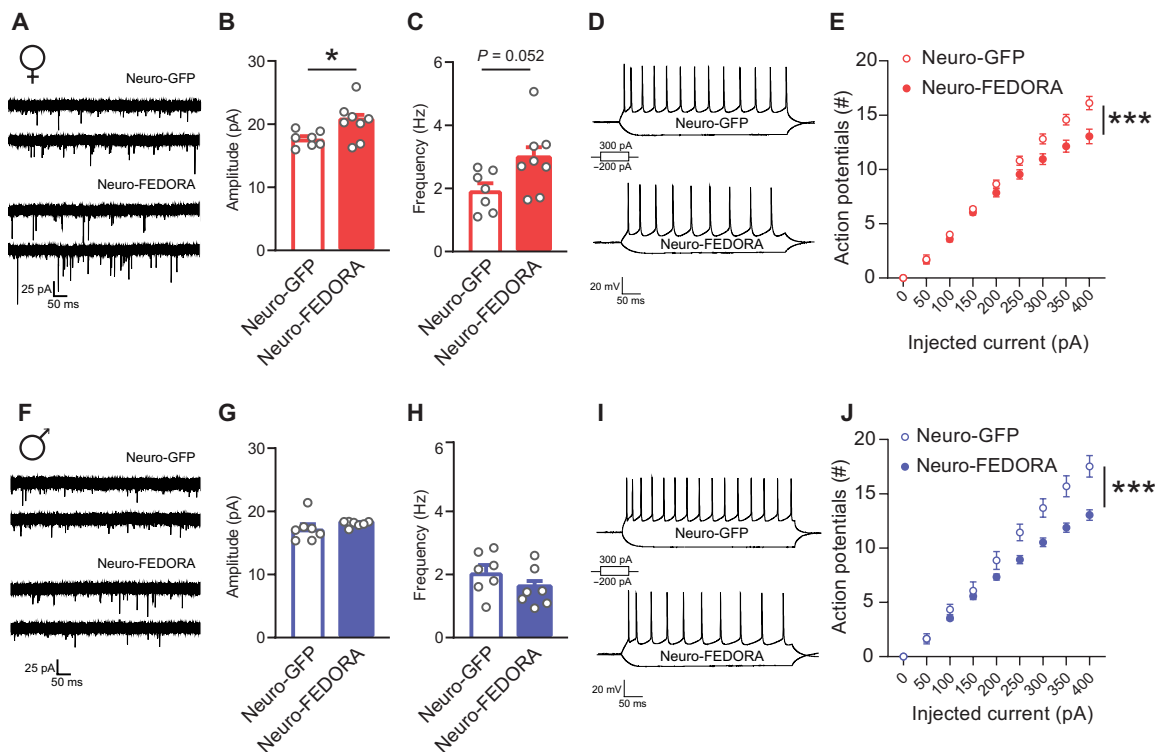


**Fig. 5. Neuronal FEDORA expression alters electrophysiological properties of mouse mPFC pyramidal neurons.** (A and F) Representative tracks of spontaneous activity from female (A) and male (F) mice expressing Neuro-FEDORA or Neuro-GFP. FEDORA expression in female neurons increased sEPSC amplitude (B) and frequency (C), with no change in males (G and H).  $n = 45$  to 58 neurons from seven to eight mice per group, Student's *t* test,  $*P < 0.05$ . Bars represent means  $\pm$  SEM, and dots represent means of individual. FEDORA expression also reduces the excitability in female (D and E) and male (I and J) pyramidal neurons. Two-way ANOVA repeated measure; main effect for virus. Recording was performed 1 day after viral infection in layer V of the infralimbic mPFC.  $n = 45$  to 58 neurons from seven to eight mice per group,  $***P < 0.001$ . Circles represent means  $\pm$  SEM.

Since MDD decreases myelin sheath thickness in PFC (27, 28), we hypothesized that this effect might be mediated by FEDORA function within oligodendrocytes. To test our hypothesis, we expressed Oligo-FEDORA or Oligo-GFP in mPFC of mice of both sexes and performed electron microscopy analysis of myelin thickness. We found that FEDORA expression decreased myelin thickness in mice of both sexes [two-way ANOVA,  $F_{virus_{1,16}} = 23.49$ ,  $P = 0.0002$ , post hoc Fisher LSD GFP (female) versus FEDORA (female)  $t_{16} = 3.034$ ,  $P = 0.0079$ ; GFP (male) versus FEDORA (male)  $t_{16} = 3.820$ ,  $P = 0.0015$ ; Fig. 6] without changing the axon diameter. This finding supports our hypothesis that FEDORA regulates myelination processes that are impaired in MDD. By contrast, FEDORA expression in oligodendrocytes had no effect on the sEPSC of mPFC pyramidal neurons (fig. S7).

To ensure that our use of HSVs to guide FEDORA expression to neurons and AAVs to guide FEDORA expression to oligodendrocytes did not confound these findings, we generated an AAV2 vector that incorporates a synapsin promoter to achieve neuron-specific FEDORA expression using AAVs. AAV-mediated FEDORA expression in female mPFC neurons increased sEPSC amplitude (GFP =  $26.29 \pm 4.2966$ ; FEDORA =  $31.24 \pm 7.600$ ; Student's  $t$  test,  $t_{26} = 2.160$ ;  $P = 0.0452$ ; 11 to 19 cells/two to three mice per group) as seen with HSVs, with no effect observed in males. Conversely, AAV-mediated FEDORA expression in male or female mPFC neurons had no effect on myelin thickness (fig. S8). Together, these findings demonstrate cell-autonomous and sex-specific effects of FEDORA on neurons and oligodendrocytes.

### Transcriptomic effects of FEDORA expression in neurons and oligodendrocytes

The ability of lncRNAs to act as epigenetic regulators of gene expression led us to the hypothesis that the sex- and cell type-specific

behavioral and cellular abnormalities induced by FEDORA are mediated by altered transcriptional regulation in the mPFC. Therefore, we characterized the female mouse mPFC transcriptome using bulk RNA-seq following the selective expression of FEDORA in either neurons or oligodendrocytes. We found that the expression of FEDORA compared to GFP had a robust effect on gene expression, leading to 2837 differentially expressed genes [DEGs; fold change > 30% and false discovery rate (FDR)-corrected  $q < 0.05$ ] when expressed in neurons (Fig. 7A) and 4037 DEGs when expressed in oligodendrocytes (Fig. 7F). As expected, cell type analysis of the DEGs revealed significant enrichment for neuronal genes for DEGs induced with Neuro-FEDORA (Fisher exact test,  $P = 2.18 \times 10^{-9}$ ) and for oligodendrocyte genes induced with Oligo-FEDORA (Fisher exact test,  $P = 7.72 \times 10^{-19}$ ; Fig. 7E). Notably, Oligo-FEDORA also significantly affected neuronal genes. Gene ontology analysis of the DEGs altered by Neuro-FEDORA highlights G protein signaling and synaptic transmission (Fig. 7B), with translation processes implicated for Oligo-FEDORA (Fig. 7G).

Next, we compared the effects of FEDORA on the mPFC transcriptome to those of CVS, which induces a similar range of anxiety- and depression-like behavioral abnormalities in female and male mice [data from (29)]. We used rank-rank hypergeometric overlap (RRHO) analysis, which compares differential expression across two datasets in a threshold-free manner (30). We found that the Neuro-FEDORA versus Neuro-GFP transcriptional signature exhibits a robust overlap with down-regulated genes of female mice exposed to CVS compared to nonstressed controls (Fig. 7C), but this was not observed for males (Fig. 7D). When we performed the same analysis on the Oligo-FEDORA versus Oligo-GFP signature, we found an opposite effect that was again more pronounced in females versus males: A significant subset of genes that were up-regulated by FEDORA expression in oligodendrocytes was down-regulated by

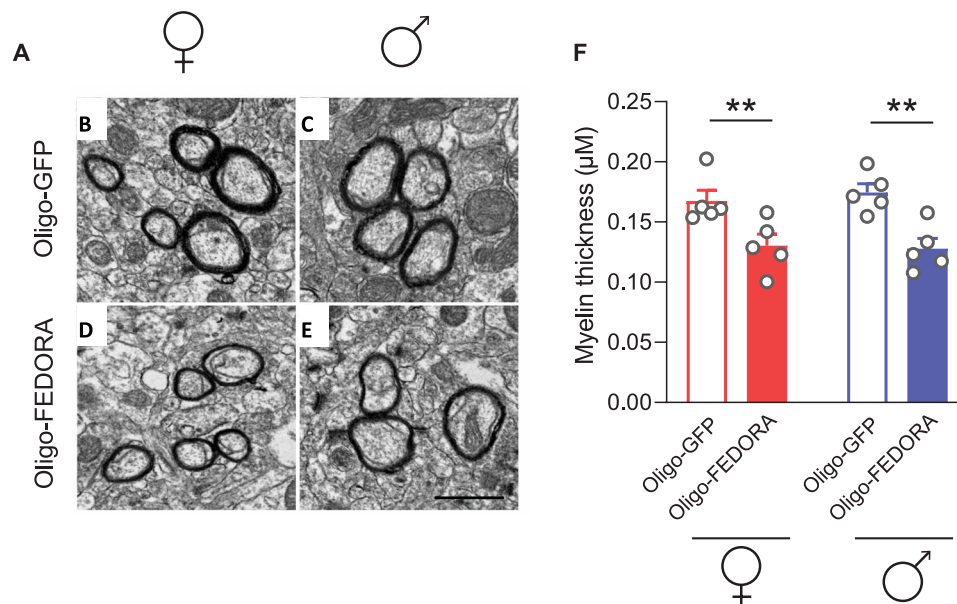


**Fig. 6. Oligodendrocyte FEDORA expression promotes myelin thinning in mouse mPFC.** (A) Representative electron microscopy (EM) images from mouse mPFC infected with Oligo-FEDORA (D and E) or Oligo-GFP (B and C) of female (B and D) or male (C and E) mice. Brains were collected 1 month after infection. Scale bar represents 1  $\mu$ M. (F) Bar graphs represent quantification of the EM pictures and indicate thinner myelin in both male and female mice expressing FEDORA compared to GFP.  $n = 91$  to 126 axons from five mice per group, two-way ANOVA, main effect for virus,  $**P < 0.01$ . Bars represent means  $\pm$  SEM, and dots represent mean of individual data.

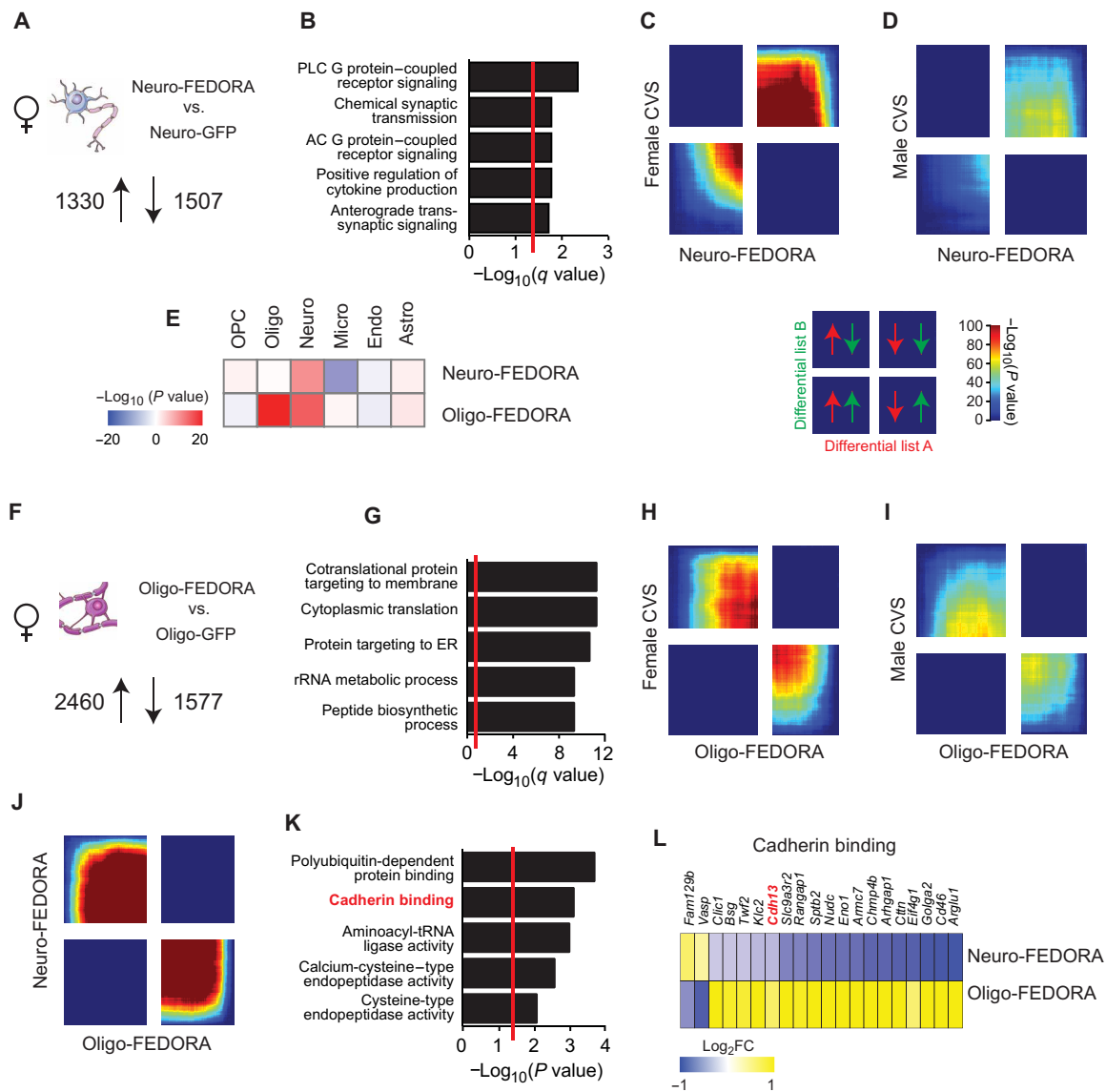


**Fig. 7. Opposing effects of FEDORA expression in neurons versus oligodendrocytes on gene expression.** (A and F) Schematic representation of bulk RNA-seq experiments in mPFC of female mice upon the selective expression of FEDORA or GFP in neurons (A) or in oligodendrocytes (F). The numbers indicate the number of genes either up- or down-regulated by FEDORA expression compared to GFP controls.  $n = 4$  to 5 samples per group ( $FC > 30\%$  and FDR-corrected  $q < 0.05$ ). (B and G) Bar graphs indicating the top biological process GO terms enriched in genes differentially expressed by Neuro-FEDORA (B) or Oligo-FEDORA (G). The red lines indicate the significance threshold at FDR-corrected  $q < 0.05$ . (C, D, H, and I) Heatmaps from an RRHO analysis (30) comparing the effects of FEDORA expression in mPFC to that of CVS on the mPFC transcriptome of mice of both sexes. Neuro-FEDORA transcriptional signature overlaps more strongly with females (C) than males (D) exposed to CVS for both co-down-regulated and co-up-regulated signals. Oligo-FEDORA displays an opposing pattern of overlap with the transcriptional signature of CVS in females (H) more so than males (I). (E) Heatmaps showing significant positive enrichment for neuronal markers in the genes differentially expressed by Neuro-FEDORA and for oligodendrocytes and, to a lesser extent, neurons by Oligo-FEDORA. Astro, astrocytes; Endo, endothall; Micro, microglia; Neuro, neurons; Oligo, oligodendrocytes; OPC, oligodendrocyte progenitor cells. (J) Heatmaps from RRHO analysis showing opposite effects on the transcriptome by Oligo-FEDORA compared to Neuro-FEDORA. (K) Bar graphs indicating the top biological process GO term enrichment analysis for genes that have opposing regulation by Oligo-FEDORA compared to Neuro-FEDORA. (L) Heatmaps highlighting the opposing regulation of the Cadherin binding genes oppositely regulated by FEDORA in the two cell types, including *CDH13*, the antisense gene of FEDORA.

CVS, and conversely, genes that FEDORA down-regulated are up-regulated by CVS (Fig. 7, H and I).

We further probed this opposite cell type-specific transcriptional effect of FEDORA and found significant enrichment for genes with a baseline sex difference in mouse mPFC [from our previous publication (29)] within the genes regulated by Neuro-FEDORA (Fisher

exact test,  $P = 2.303 \times 10^{-14}$ ) and Oligo-FEDORA (Fisher exact test,  $P = 0.202$ ; fig. S9A). Specifically, numerous genes that are expressed at higher levels at baseline in females versus males are down-regulated upon Neuro-FEDORA expression (fig. S9B). Moreover, we found a cell type-specific effect of FEDORA on the expression pattern of the 360 PCGs that significantly correlate with FEDORA in our female

human postmortem brain dataset (fig. S9C). Next, we directly compared the Neuro-FEDORA to the Oligo-FEDORA transcriptional profiles and found a strong inverse effect on gene expression between the cell types (Fig. 7J). Gene ontology analysis of the genes demonstrating this opposite regulation highlights protein binding, particularly cadherin binding (Fig. 7K). One of these genes is *Cdh13* (Fig. 7L), the gene to which FEDORA is antisense. Together, these results suggest that FEDORA promotes opposing cell type-specific patterns on gene expression and implicate its host gene, *Cdh13*, as one potential mediator of these effects.

### FEDORA levels in human blood track MDD symptoms in females

Last, we tested the translational potential of the sex-specific regulation of FEDORA by testing whether its circulating levels may serve as a diagnostic or prognostic biomarker for female MDD. We probed total blood levels of FEDORA in a cohort of MDD cases of both sexes compared to matched HCs. The cases were treatment-resistant patients enrolled in a study in which they were treated with the rapidly acting antidepressant ketamine, and blood was recollected 24 hours after treatment (Fig. 8A). We performed qPCR to probe the levels of

FEDORA and found that its expression levels were higher in females with MDD compared to HCs before treatment [two-way ANOVA,  $F$  group<sub>2,100</sub> = 4.523,  $P$  = 0.0132, post hoc Fisher LSD HC (female) versus MDD-pre (female)  $t_{100}$  = 2.666,  $P$  = 0.0089; Fig. 8B]. This effect was not apparent in males. Ketamine treatment did not normalize the levels of FEDORA at the group level. However, we found a significant correlation between the change in FEDORA expression at pretreatment to posttreatment time points and the change in depression severity as measured by the Quick Inventory of Depressive Symptomatology (QIDS) in female MDD subjects (Pearson correlation,  $r$  = 0.605;  $P$  = 0.0377; Fig. 8C), but not in males (Fig. 8D). Notably, there were no significant correlations between FEDORA blood levels and the demographic characteristics of either of the cohorts (fig. S10). Together, these results suggest that FEDORA total blood levels may serve as a female-specific diagnostic tool for MDD, which tracks treatment response to ketamine in females.

### DISCUSSION

Here, we report that lncRNAs exhibit a notable sex difference in expression across the brain of healthy individuals and that this

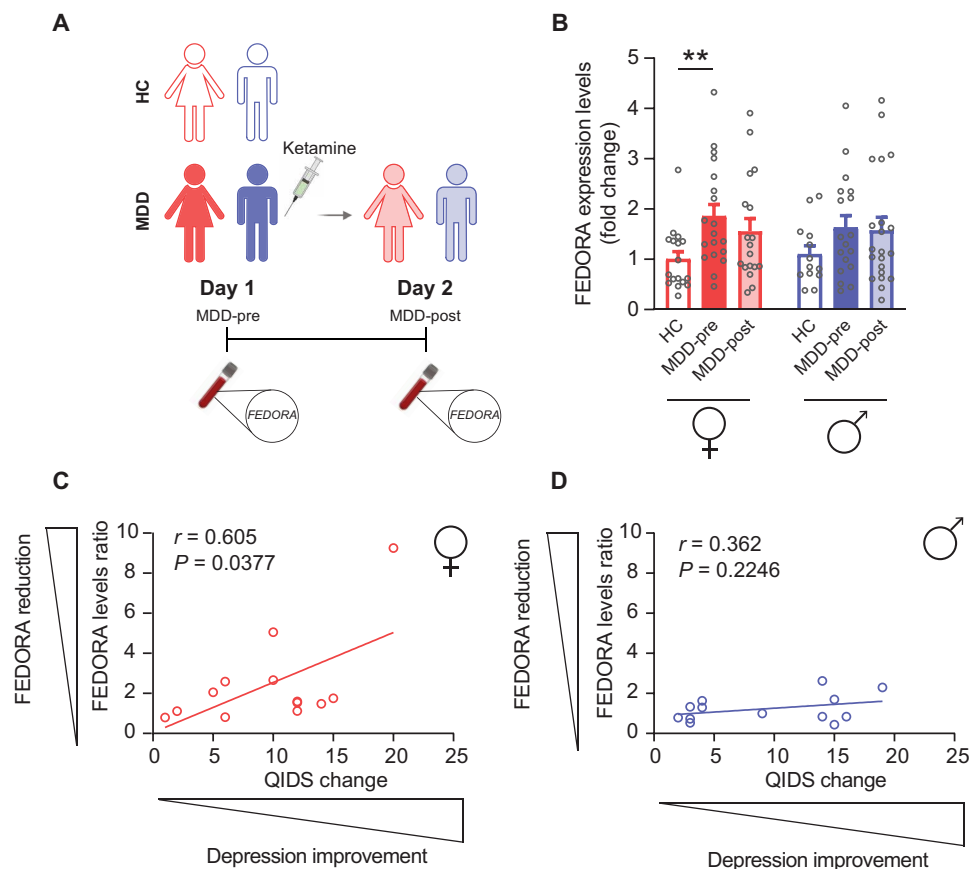


**Fig. 8. Blood FEDORA levels are associated with MDD symptoms and response to ketamine treatment in females only.** (A) Schematic representation of the experimental design. Blood was collected from treatment-resistant MDD (MDD-pre) and HC subjects of both sexes. MDD subjects were treated with the fast-acting antidepressant ketamine, and blood was drawn again 1 day later (MDD-post) along with clinical assessment. (B) Bar graph showing that blood levels of FEDORA as measured by qPCR are higher in MDD-pre females compared to HCs, but not in males.  $n$  = 13 to 21 per group, Fisher LSD post hoc,  $**P < 0.01$ . Bars represent means  $\pm$  SEM, and dots represent individual data points. (C and D) Graphs demonstrating the correlation between the change in MDD-post versus MDD-pre in FEDORA levels and the change in the QIDS scale. There is a significant positive correlation between the improvement in MDD and the reduction of FEDORA levels in female (C), but not male (D), subjects.  $n$  = 15 to 16 per group.

sex-specific pattern of expression is broadly lost in patients diagnosed with MDD. We highlight one such lncRNA, which we named FEDORA, after demonstrating that it is up-regulated across cortical brain regions in females, but not males, with MDD compared to HCs in two independent cohorts. By expressing FEDORA selectively in neurons or in oligodendrocytes of mouse mPFC, we validated its role as a sex-specific mediator of anxiety- and depression-like behavior. We also demonstrate a cell type-specific influence of FEDORA on neuronal and oligodendrocyte function: FEDORA alters synaptic physiology when expressed in neurons with no effect seen upon expression in oligodendrocytes, alters myelin thickness in oligodendrocytes, and promotes opposite transcriptional programs in these two cell types. This exogenous expression of FEDORA in mPFC neurons is sufficient to promote a transcriptional signature that resembles that seen in the mPFC of chronically stressed female mice. These transcriptional effects of FEDORA are mediated presumably by epigenetic mechanisms, an important focus of future work. The transcriptional changes induced by expressing FEDORA in neurons and oligodendrocytes implicate regulation of the cell adhesion molecule CDH13 to which FEDORA is an antisense transcript. Last, we show that blood levels of FEDORA reflect depression diagnosis specifically in women and correlate with the extent of their response to ketamine treatment. Together, these results highlight the role of lncRNAs in maintaining the transcriptional homeostasis underlying sex differences in the brain and point to FEDORA as a diagnostic and therapeutic target for depression in women.

Sex differences have emerged as critical mediators of stress, anxiety, and depression in recent years (31), and several lines of evidence suggest that males and females exhibit mostly distinct patterns of transcriptional regulation throughout limbic brain regions in MDD in humans and after chronic stress in mice (21, 26, 29, 32). Here, we report that MDD erases transcriptomic sex differences typically observed in HCs across brain regions associated with depression. This phenomenon, replicated in an independent cohort, is similar to what we observed in the brains of adult mice that were exposed to social isolation in adolescence (33). We speculate that chronic stress suppresses the transcriptional processes that help maintain baseline homeostatic sex differences, which are thought to support cognitive, emotional, and behavioral strategies that are used differently by males and females. In depressed subjects, this balance is disrupted, which contributes to the abnormalities seen in depression. We note that the loss of sex differences in MDD is more pronounced for lncRNAs compared to PCGs. We hypothesize that lncRNA expression levels are less tightly regulated compared to PCGs; therefore, lncRNAs are more responsive to environmental factors such as stress. As a result, the effects of the environment on expression levels of PCGs are buffered by multiple regulatory factors, including lncRNAs, leading ultimately to smaller effect sizes.

There are reports of a sex-specific expression pattern of lncRNAs in mammalian gonads (23) and mouse liver (34, 35) and in the brain of zebrafish (36) and drosophila (37). Specific lncRNAs such as the maternally imprinted *Peg13* were linked to regulating behaviors and gene expression (38), whereas *Xist* is associated with female-specific X chromosome inactivation (39) and sex-specific gene expression silencing (40). There are reports that sex-biased lncRNA expression in the liver associates with sex-biased accessible chromatin regions and hormonal binding sites (34); however, the processes that guide baseline sex differences in lncRNA expression in the brain remain unknown, particularly as they relate to altered expression patterns

in MDD. We speculate that these sex differences in brain lncRNA expression patterns are mechanistically linked to genetic differences between the sexes, rather than to sex hormones, as we find elevated levels in FEDORA in the mPFC of depressed women across the spectrum of fertility and menopause.

FEDORA is antisense to *Cdh13* mRNA, which encodes a member of the cadherin superfamily of cell adhesion molecules and is expressed predominantly in neurons and in oligodendrocyte progenitor cells and mature oligodendrocytes (41). In neurons, CDH13 is localized to the cell membrane, where it acts as a negative regulator of axon growth during neuronal differentiation. Genetic studies have linked variations in *CDH13* to diagnosis with attention deficit hyperactivity disorder, alcohol dependence, and MDD (42–45). Moreover, a recent proteome-wide association postmortem brain study of MDD reported CDH13 as a significant hit (46). Notably, another cadherin family member, protocadherin 19, has been suggested to exhibit a female-specific role in synaptic and cognitive function (47). While CDH13 is not regulated in MDD at the RNA level in our postmortem human brain dataset nor in mouse models of chronic stress (29, 48), we found a robust opposite regulation of *Cdh13* upon expression of FEDORA in neurons versus oligodendrocytes. This opposing regulation is part of the genome-wide cell type-specific opposite-effect of FEDORA on the transcriptome in these cell types. These findings warrant further investigation of CDH13 as a potential mediator of some of FEDORA's effects on the brain under normal and pathological conditions.

We report here that neuronal expression of FEDORA in mPFC promotes anxiety- and depression-like behavioral abnormalities. Our findings align with a large body of literature indicating that neuronal dysfunction in the PFC, the central hub of executive functions, contributes importantly to MDD. There are reports from postmortem brain studies from MDD subjects (49, 50) and rodent chronic stress models (51, 52) describing the loss of synapses, a decrease in synaptic-related genes, and alterations in mPFC neuronal electrophysiological properties. Similarly, we found that neuronal expression of FEDORA promotes altered expression of synaptic genes along with changes in neuronal excitability. Notably, our current results that FEDORA-induced behavioral abnormalities in females coincides with increased amplitude and frequency of sEPSCs of mPFC pyramidal neurons are in line with our former study of another lncRNA, LINC00473, which promotes female-specific stress resilience and opposite effects on sEPSCs (17), and with reports on sex- and pathway-specific effects of chronic stress on mPFC physiology (53). Collectively, our study adds FEDORA as a mediator of the female brain's molecular arsenal that controls mPFC excitability and that is aberrantly expressed in MDD.

Multiple studies have found deleterious effects of MDD on oligodendrocytes and myelination in the PFC [reviewed in (54, 55)], reporting lower density of oligodendrocytes in MDD cases (56, 57), white matter abnormalities, and down-regulation of oligodendrocyte genes (58–61). Rodent studies using several chronic stress models report reduced oligodendrocyte proliferation and thinning of myelin in the PFC, which was reversed by antidepressant treatment (62–68). Consistent with these findings, we show that FEDORA expression in oligodendrocytes produced a prodepressive-like behavioral effect, although the behavioral abnormalities induced by oligodendrocyte FEDORA expression are different from those induced by neuronal FEDORA expression. FEDORA expression in oligodendrocytes also caused thinning of myelin in the mPFC. Notably,

while the prodepressive behavioral effects were only apparent in female mice, we noted myelin thinning in both sexes. This lack of sex specificity aligns with the decreased intrinsic (as opposed to synaptic) excitability that we report in neurons from mice of both sexes upon FEDORA expression in neurons. We speculate that these two phenomena may be interrelated, as decreased myelin thickness can alter neuronal excitability (69–71). In addition, we found enrichment for altered expression of synaptic and postsynaptic genes when expressing FEDORA in female mice in neurons (fig. S9D) or in oligodendrocytes (fig. S9E). We speculate that reciprocal interactions between oligodendrocytes and neurons support dynamic plasticity in the thickness of myelin sheaths regulated by FEDORA, potentially through its interaction with CDH13. Alternatively, in line with evidence for aberrant chromatin structure in oligodendrocyte progenitor cells within the PFC of chronically stressed mice (67), we hypothesize that FEDORA may regulate chromatin structure, as often is the case with lncRNAs, to direct transcriptional processes leading to prodepressive effects.

We also report that the sex-specific differential regulation of FEDORA in the brains of patients with MDD is observed in the circulation, with higher FEDORA levels observed in whole blood of treatment-resistant depressed females, but not males. Although previous studies have profiled the genome-wide transcriptional changes in blood of individuals with MDD compared to HCs (72–74), none has included sex as a biological variable. We also identified a correlation between reductions in FEDORA blood levels by treatment with ketamine and its therapeutic efficacy. Future studies are required to determine whether this effect is specific to ketamine or is generalized to other classes of antidepressants such as selective serotonin reuptake inhibitors. While rodent studies report heightened sensitivity to ketamine in females [reviewed in (75, 76)], meta-analyses of human studies did not find sex differences in the effects of acute ketamine treatment for MDD (77, 78). It is unclear whether the mechanisms that lead to up-regulation of FEDORA in the brain of depressed women are similar to those that alter its expression in the circulation. FEDORA is expressed predominantly in antibody-producing B cells in blood (79). Most studies to date on circulating factors in the context of stress and depression focus on the innate immune system or T cell-related processes and not on B cells (80); therefore, our unique finding of a B cell-specific depression biomarker is interesting and warrants further investigation. Similar to most of the lncRNAs, FEDORA blood levels are relatively low, a challenge that needs to be addressed in its biomarker development.

To conclude, our findings support the view that human-specific lncRNAs serve a prominent regulatory role in higher brain function, including mood, under normal and pathological conditions. We acknowledge that mechanistic studies of the role of a human-specific transcript such as FEDORA in the context of a complex brain disorder present many challenges. However, although mice do not express FEDORA or any apparent homolog, we hypothesized that FEDORA would nevertheless produce specific effects in mice based on the knowledge that many lncRNAs act by binding to DNA, RNA, or protein targets and that mice likely express many of FEDORA's targets even if they do not express FEDORA itself. The marked sex- and cell type-specific effects induced by FEDORA expression in neurons or in oligodendrocytes support this hypothesis. In addition, our approach of expressing a human-specific lncRNA in mice has successfully been used by us and other groups to understand the actions of other lncRNAs in brain and other tissues (17, 81, 82). We

speculate that human-specific lncRNAs such as FEDORA arose later in evolution as an additional layer of regulation of increasingly complex molecular pathways already established in earlier mammals such as mice. Our findings with FEDORA support this possibility and elaborate previously unknown molecular mechanisms that contribute to sex differences in higher brain function at baseline and in the context of MDD.

## MATERIALS AND METHODS

### Animals

Experiments used 8-week-old C57BL/6J male or female mice (the Jackson Laboratory). Mice were habituated to the animal facility for 1 week before any manipulations and were maintained at 23° to 25°C with a 12-hour light/12-hour dark cycle (lights on at 7:00 a.m.) with ad libitum access to food and water. Experiments were conducted following the guidelines of the Institutional Animal Care and Use Committee at Mount Sinai.

### Behavioral testing

Mice treated with the Neuro-FEDORA or Neuro-GFP were allowed 3 days to recover from surgery before 2 days of behavioral testing consisting of three tests a day to fit within the short expression window of HSVs. For Oligo-FEDORA and Oligo-GFP experiments, we waited 30 days between surgery and behavioral testing to allow maximal transgene expression, and mice were tested with one to two tests a day.

### Novelty-suppressed feeding

The novelty-suppressed feeding test assesses anxiety- and depression-related behaviors (83). Mice were food-deprived for 24 hours before testing and habituated to the experimental room for 1 hour before testing. Mice were placed in the corner of a box (50 cm by 50 cm by 20 cm) covered with bedding with a single food pellet placed in the center of the arena. The latency to eat was recorded under red light conditions during 5 min of testing. Mice were then transferred to their home cage, and their latency to eat was recorded there as well.

### Sucrose preference

Mice were housed individually and given a choice between two 50-ml conical tubes with either water or 1% sucrose solution for 24 hours (84). The bottles were weighed, and sucrose preference was calculated by determining the percentage of sucrose consumption divided by total liquid intake over 1 day. Total liquid intake did not differ across experimental groups studied.

### Elevated plus maze

For the elevated plus maze, which assesses anxiety-related behavior (85), mice were acclimated to the testing room for 1 hour before testing. Animals were tested in a cross-shaped maze consisting of two 12 cm-by-50 cm open arms and two closed arms with 15-cm-high walls under red light for 5 min. Behavior was tracked using an automated system (EthoVision, Noldus).

### Marble burying

The marble burying test for anxiety-related behaviors (86) was conducted under red light conditions. After 1 hour of acclimation to the testing room, mice were put in a standard mouse cage filled

with 15 cm of corn cob bedding topped with 20 glass marbles. After 15 min, the mice were removed, and the number of marbles fully or partially buried were counted.

### Forced swim test

The forced swim test, which assesses an animal's response to an acute stress, was performed after 1 hour of habituation to the testing room. Mice were tested in a 4-liter glass beaker, containing 3 liters of water at  $25^{\circ} \pm 1^{\circ}\text{C}$  for 6 min under white light conditions. The behavior was video-tracked using an automated system (EthoVision, Noldus) (84).

### Tail suspension test

The tail suspension test was performed following 1 hour of habituation to the testing room. Mice were taped from their tail for a 10-min video recorded trial. Time spent immobile and latency to eat first was manually scored by an observer blind to the mice group.

### Open field test

The open field test was performed following 1 hour of habituation to the testing room. Mice were placed in a white box apparatus (50 cm by 50 cm by 40 cm) for 10 min, and their behavior was video-tracked and analyzed using an automated system (EthoVision, Noldus).

### Operant lever press task

Mice were trained to lever-press for a liquid saccharin reward in operant conditioning boxes (22 cm by 18 cm by 13 cm; Med Associates, St Albans, Vermont) as described previously (87). Each box contained two levers and a motor-driven dipper that delivers 0.02 ml of 0.2% saccharin through a hole in the magazine floor per correct lever press. Operant boxes were illuminated and enclosed in a sound-attenuating chamber equipped with a ventilation fan. Training started 1 month after surgery that delivered Oligo-FEDORA or Oligo-GFP to the mPFC. Female and male mice were tested separately and acclimated to water restriction and saccharin for 3 days in their home cage and then maintained on water restriction (2-hour ad libitum access per day) throughout testing. First, mice were trained to retrieve saccharin from the reward magazine when it was presented. During the training, the shift to the next task or schedule was carried out after the behavior stabilized. Next, in 30-min daily sessions, mice were trained to lever press for saccharin on an FR1 schedule of reinforcement, in which each correct lever press is rewarded, for 6 days. This was followed by an FR2 for 4 days, an FR5 for 4 days, and lastly a schedule of RR5 reinforcement with a one-in-five chance of the response being rewarded for 5 days.

### Chronic variable stress

A subthreshold shortened CVS protocol was used to induce depression- and anxiety-like behavior with a timeline that matches the expression of HSVs (26, 29). The protocol consists of exposure to three different stressors over a period of 3 days. The female mice were exposed to one of the following stressors for 1 hour daily: 100 random mild foot shocks at 0.45 mA, a tail suspension, or restraint stress within a ventilated 50-ml conical tube. Mice were group-housed during the stress exposure and individually housed during the behavioral assessment. Unstressed mice were used as controls. Neuro-FEDORA and Neuro-GFP female mice started the exposure to this subthreshold CVS protocol 1 day after stereotactic surgery, followed by behavioral testing.

### Viral vectors

For neuronal expression, FEDORA was synthesized (Gene Script) and Gateway (Invitrogen)-cloned into a p1005<sup>+</sup> HSV vector. This vector expresses enhanced GFP (eGFP) with a cytomegalovirus promoter, while the gene of interest is driven by the IE4/5 promoter. Empty p1005<sup>+</sup> expressing eGFP only was used as the control. The plasmids were packaged into HSVs that are highly neurotrophic (25) and display rapid induction; therefore, experiments were performed 3 days after infection, with equivalent effects seen in male and female mice. For oligodendrocyte expression, FEDORA was subcloned into pAM/0.3KB-MAG-eGFP AAV vector, contributed by M. Klugmann (University of New South Wales, Australia). The plasmid includes a 0.3-kB truncated form of the promoter of the human MAG gene that drives transgene expression in oligodendrocytes (88) and fits within AAV plasmid size constraints. Empty pAM/0.3KB MAG-eGFP expressing eGFP only was used as the control. The plasmids were used to make AAV1 serotype at the vector core of the University of Pennsylvania at a concentration of  $10^{13}$  genome copies/ml. Separate AAV vectors, using AAV2 serotype with incorporation of the synapsin promoter, were used to target AAV transgene expression to neurons. Experiments using these AAV tools were performed 1 month following mPFC infection when transgene expression is maximal. Validation of HSV and AAV vectors was confirmed by epifluorescence microscopy and qPCR, with equivalent effects seen in male and female mice.

### Stereotactic surgery

Mice were anesthetized with a mixture of ketamine (100 mg/kg) and xylazine (10 mg/kg) and positioned in a small-animal stereotactic instrument (Kopf Instruments). The skull surface was exposed, and 33-gauge syringe needles (Hamilton) were used to bilaterally infuse 0.5  $\mu\text{l}$  of viral vectors at a rate of 0.1  $\mu\text{l}/\text{min}$ . mPFC coordinates relative to the bregma were as follows: anterior posterior, +1.8 mm; medial lateral, +0.75 mm; and dorsal ventral, -2.7 mm with 15° angle. Independent cohorts of mice were used for validation, behavioral, electrophysiological, morphological, and transcriptional analyses.

### Electrophysiology

Pyramidal neurons in layer V of the infralimbic mPFC of male and female mice were studied in brain slices 1 day after mice received intra-mPFC injections of Neuro-FEDORA or Neuro-GFP. Parallel experiments were performed 30 days after intra-mPFC injection of Oligo-FEDORA or Oligo-GFP or of the neuron-targeting AAV vectors. Virally infected neurons were distinguished from noninfected neurons by their GFP signals under epifluorescence microscopy. sEPSCs were recorded for 3 min in the voltage-clamp mode, with a K-based internal solution [130 mM K-methanesulfonate, 10 mM KCl, 10 mM Hepes, 0.4 mM EGTA, 2.0 mM  $\text{MgCl}_2$ , 3 mM MgATP, 0.5 mM  $\text{Na}_3\text{GTP}$ , 7.5 mM phosphocreatine, (pH 7.4; 285 mOsm)]. The frequency and amplitude of sEPSCs were analyzed with Mini Analysis Program (Synaptosoft).

### Electron microscopy

Male and female mice were perfused as described previously (67) for electron microscopy analysis 1 month after stereotactic delivery of AAVs expressing FEDORA or GFP ( $n = 4$  to 5 per group), using AAVs that target oligodendrocytes versus neurons selectively. Brains were harvested and vibratome-sectioned into 60- $\mu\text{m}$  slices containing the mPFC. Sections were resin-embedded, thin-sectioned at 90 nm,

stained with uranyl acetate and lead citrate, and mounted on 200-mesh copper grids. Ten images at 10,000 $\times$  were collected per mouse using a transmission electron microscope JEOL JEM 1400Plus equipped with a Gatan charge-coupled device camera. ImageJ was used to measure both axon caliber and myelin fiber diameter for about 100 myelinated axons per mouse. All analyses were performed blind to the experimental conditions.

### Immunohistochemistry, imaging, and cell counting

Adult mice were terminally anesthetized with ketamine/xylazine (Neuro-FEDORA, 3 days after infection; Oligo-FEDORA, 30 days after infection) and transcardially perfused with PBS followed by 4% paraformaldehyde, and brains were postfixed in 4% paraformaldehyde at 4°C. Coronal sections (30  $\mu$ m) were sliced on a vibratome, washed 3 $\times$  with PBS 0.1% Triton-X (PBST), and blocked with normal donkey serum (3%) at room temperature for 1 hour in PBST. Sections were then incubated in primary antibodies overnight at 4°C in blocking solution [1:2000 Chicken Anti-GFP (#GFP-1020, Aves Labs), 1:500 Rabbit Anti-Olig 2 (#AB9610, Abcam), Rabbit Anti-GFAP (#ab7260, Abcam), and Rabbit Anti-Neun (#NBPI-77686, Novus)]. Sections were then washed 3 $\times$  in PBS and incubated with secondary antibodies [1:500 Alexa 488 Donkey Anti-Chicken (#703-546-155, Jackson ImmunoResearch) and 1:500 Cy3 donkey anti-rabbit (#711-166-152, Jackson ImmunoResearch)] for 90 min at room temperature. Sections were washed in PBS, mounted on slides, and coverslipped with ProLong Gold with Antifade including 4',6-diamidino-2-phenylindole (DAPI; Invitrogen). For quantification of immunohistochemistry, slides were imaged on a Zeiss LSM 710 confocal microscope. Only high-quality slices at a similar level along the A-P axis were imaged at  $\times$ 20 magnification, such that three to four slices per mouse were imaged and quantitated ( $n = 3$  to 5 mice per marker). Analysis of cell counts and colocalization was performed using ImageJ by an observer blind to condition. Fluoro-Jade was used as a marker of cell necrosis on separate tissue sections using published procedures. A mean count per mouse was used for statistical analysis.

### Human postmortem situ hybridization

Fluorescent in situ hybridization (FISH) was performed on an independent cohort of male and female MDD cases ( $n = 10$  per group; table S2). The samples were obtained by The University of Texas Southwestern Medical Center at Dallas with consent from the next of kin. Collection criteria included <24-hour postmortem interval (PMI) and no direct head trauma or other medical illness. The brains were taken from the skull, put on ice, dissected, and flash-frozen. Samples were stored at  $-80^{\circ}\text{C}$  in plastic under a vacuum seal. The diagnosis was performed on the basis of hospital and medical records and interviewer with the next of kin. This information was reviewed by four clinicians that came to a consensus diagnosis using Diagnostic and Statistical Manual of Mental Disorders, Fourth Edition (DSM-IV) criteria. Subjects were matched to controls for age, pH, RNA integrity number (RIN), and PMI.

FISH was performed using RNAscope in human rACC in layers II to VI for gray matter and from subcortical white matter. Fixed frozen tissue samples were cryostat-sectioned (14  $\mu$ m) and mounted on Superfrost Plus slides. The RNAscope Multiplex Fluorescent Reagent Kit and probes for FEDORA (LOC105371366), as well as RNA binding protein, fox-1 homolog 3 (neuronal marker), oligodendrocyte transcription factor 2 (oligodendrocyte makers), and fluorophore [tyramide amplification kits (TSA)], were used according to

the manufacturer's instructions. Briefly, the slides were subjected to pretreatment, including hydrogen peroxide, epitope retrieval in 100°C water bath, and digestion enzyme. Next, the sections received FEDORA probes and were hybridized for 2 hours at 40°C. Amplification and detection were performed using TSA Fluorescein (1:750) before counterstain with DAPI. Confocal images were acquired using a Zeiss LSM 800 confocal microscope. High-resolution and high-magnification tiling images were taken from the region of interest (ROI). Quantification was performed with Fiji/ImageJ (National Institutes of Health). The number of puncta was extracted, and density was calculated by dividing the size of the ROI.

### RNA extraction

To collect FEDORA expressing mPFC samples, mice were cervically dislocated, and the brains were rapidly removed. Neuro-FEDORA tissue was collected 3 days after infection, and Oligo-FEDORA was collected 30 days after infection. Bilateral 1-mm-thick 14-g microdissections of mPFC were taken from fresh slices and flash-frozen on dry ice. Total RNA was isolated with QIAzol (QIAGEN) and purified with the RNeasy Micro Kit (QIAGEN), including on-column deoxyribonuclease (DNase) treatment. For human subjects' blood, intravenous blood was collected using EDTA tubes and stored in a  $-80^{\circ}\text{C}$ . Total RNA was extracted using the Total RNA Purification Kit (Norgen Biotek) including on-column DNase treatment. All samples were tested for concentration and purity using a NanoDrop (Thermo Fisher Scientific). Samples used for RNA-seq were analyzed using a Bioanalyzer RNA Nano chips (Agilent) for integrity.

### Reverse transcription and qPCR

RNA amount was normalized across samples, and cDNA was created using iScript (Bio-Rad). Real-time PCR reactions were run in triplicate, and SYBR-green was used in a QuantStudio 7 (Thermo Fisher Scientific) qPCR machine. The  $2^{-\Delta\Delta\text{Ct}}$  method was used to calculate relative gene expression normalized to controls with *Hprt1* as the house-keeping gene. cDNA was diluted to a concentration of 3 ng/ $\mu$ l for qPCR reactions, and FEDORA was detected in vmPFC in control samples with mean cycle threshold (Ct) values of  $32.1 \pm 1.2$  and  $27.8 \pm 0.9$  in the blood, while HPRT1 mean Ct values in the brain were  $28.26 \pm 1.2$  and  $30.2 \pm 0.3$  in the blood. See table S4 for primer sequences.

### Sequencing library preparation

RNA libraries were prepared from female mouse mPFC infected with Neuro-FEDORA or Neuro-GFP and from Oligo-FEDORA or Oligo-GFP. The successful manipulation of FEDORA was confirmed in the samples used for sequencing by qPCR. Libraries were made using 1  $\mu$ g of purified RNA for neuron sequencing using the ScriptSeq Complete Kit (Epicentre) and 500 ng of RNA for oligodendrocyte with the TruSeq Stranded Total RNA (Illumina). Library preparation kits were changed because of discontinuous production of the Epicentre kit. For library preparation, the cDNA was synthesized from ribosomal-depleted RNA and then fragmented total RNA using random hexamers, followed by terminal tagging. The libraries were PCR-amplified and then purified using AMPure XP beads (Beckman Coulter). Barcode bases were introduced at the end of the adaptors during PCR amplification steps. Quality and concentration of libraries were confirmed on a Bioanalyzer (Agilent), and libraries were sequenced on an Illumina HiSeq machine with 150-bp paired-end reads by Genewiz. Samples were multiplexed to produce >50 million reads per sample. Sample size was  $n = 4$  to 5 independent samples per group.

## RNA-seq analysis of human postmortem brain and mouse brain

Human postmortem RNA-seq data from MDD and HC were collected, analyzed, and reported as part of a published study (29). Briefly, brain tissue was obtained from the Douglas Bell Canada Brain Bank, Québec. Males and females were group-matched for age, pH, and PMI. Subject information is listed in table S1. Inclusion criteria for both cases and controls were French-Canadian European origin and sudden death. Forty-eight subjects were recruited, and tissue was collected from six brain regions: the OFC (BA11), dlPFC (BA8/9), cingulate gyrus 25 (vmPFC; BA25), aINS, NAc, and vSUB. The study was approved by the research ethics boards of McGill University. In addition to phenotype (MDD versus HC), sex and brain region, RIN, age, and alcohol had a significant effect on the overall variance in the dataset, whereas antidepressant use did not. All of these factors (but sex) were included in the statistical models as covariates. By contrast, other drugs, cause of death, history of child abuse, or other early life adversity and toxicology findings were not associated significantly with global variance of gene expression.

Sex differences were studied on the basis of the differential expression analyses between HC females and males by brain region, which was part of the original RNA-seq study (29), as well as in the independent cohort (21). Here, we filtered these lists to identify genes with baseline sex differences with fold change > 30% and nominal  $P < 0.05$ . We define a loss of baseline sex differences if an RNA that is up-regulated in HC females compared to males is down-regulated in females with MDD compared to female HC (fold change > 30%) or up-regulated in male MDD compared to male HC, or the inverse patterns, RNA that is down-regulated in HC females compared to males is up-regulated in females with MDD compared to female HC or down-regulated in male MDD compared to male HC. We also only included lncRNAs in our analyses that lost their baseline sex difference only in one of the sexes and not in both.

The correlation analysis between lncRNA and PCG expression data was part of our former study (17), where we performed genome-wide Pearson correlation between the brain site-normalized expression level (logCPM) of an lncRNA and PCG for each sex separately. Permutation analysis of the same number of random genes iterated 10,000 times was used to calculate a threshold for significant Pearson correlation at  $R > 0.58771$  or  $R < -0.59516$ , with 23% FDR.

For RNA-seq differential expression analysis, raw reads were aligned to the mouse genome (mm10) using Hierarchical Indexing for Spliced Alignment of Transcripts 2 (89). The average mapping rates for neurons and oligodendrocytes were 84 and 89%, respectively. Quality control was performed using FastQC (90), and principal components analysis was used to identify outliers. Normalization and differential expression analysis were performed using DESeq2 (91). Raw data were deposited in GEO (GSE188930). Significance was set at FDR-corrected  $q < 0.05$ , and a fold change threshold was set at >1.3. See tables S7 and S8 for Neuro-FEDORA and Oligo-FEDORA differential gene expression lists, respectively. Heatmaps were generated using Morpheus (<https://software.broadinstitute.org/morpheus>). Gene ontology analysis for enrichment of biological process was performed using Enricher (92), and SynGo was used to analyze synaptic genes enrichment (93). Cell type enrichment analysis was performed by comparing the DEG signature to a mouse brain cell type-specific marker lists (94) followed by a Fisher exact test. RRHO analysis was used to evaluate the overlap of differential expression lists between Neuron-FEDORA or Oligo-FEDORA expression and

mouse CVS signature from our published dataset (29). A two-sided version of this analysis was used to test for coincident and opposite enrichment (30).

## Human blood study

Male and female participants between the ages of 18 to 65 were recruited through the Depression and Anxiety Center for Discovery and Treatment at the Icahn School of Medicine at Mount Sinai for a ketamine study (95, 96). The diagnosis was assessed using the structural clinical interview for the DSM-V. Participants met diagnostic criteria for a current major depressive episode of at least moderate severity as measured by the Clinical Global Impression-Severity Scale (CGI-S), as well as a lifetime history of nonresponse to at least two trials of antidepressants. Demographic information (table S3), as well as an additional psychiatric evaluation, was collected within 28 days before the initial blood draw. Exclusion criteria included a lifetime history of a psychotic disorder, bipolar disorder, alcohol or other substance abuse (confirmed by urine toxicology), any unstable medical condition, any systemic inflammatory or autoimmune disease, current antidepressant use, and pregnancy or nursing. MDD severity at baseline was measured using the QIDS, after which blood samples were collected. Thereafter, participants received a single ketamine intravenous infusion of 0.5 mg/kg over 40 min. One day after the infusion, both MDD severity scores and blood samples were collected again. The study was approved by the program for the protection of human subjects at Mount Sinai, and participants provided informed consent.

## Statistical analyses

All statistics were performed using Prism 9. Outliers were defined as more than 2.5 SDs from the group mean and were removed from the analysis. Main effects and interactions were determined using two-way ANOVA including repeated measures when needed with Fisher LSD post hoc analysis. Student's  $t$  test was used for comparisons of only two groups. All significance thresholds were set at  $P < 0.05$ .

## SUPPLEMENTARY MATERIALS

Supplementary material for this article is available at <https://science.org/doi/10.1126/sciadv.abn9494>

[View/request a protocol for this paper from Bio-protocol.](#)

## REFERENCES AND NOTES

1. S. Seedat, K. M. Scott, M. C. Angermeyer, P. Berglund, E. J. Bromet, T. S. Brugha, K. Demmyttenaere, G. de Girolamo, J. M. Haro, R. Jin, E. G. Karam, V. Kovess-Masfety, D. Levinson, M. E. Medina Mora, Y. Ono, J. Ormel, B. E. Pennell, J. Posada-Villa, N. A. Sampson, D. Williams, R. C. Kessler, Cross-national associations between gender and mental disorders in the World Health Organization World Mental Health Surveys. *Arch. Gen. Psychiatry* **66**, 785–795 (2009).
2. G. S. Malhi, J. J. Mann, Depression. *Lancet* **392**, 2299–2312 (2018).
3. H. Akil, J. Gordon, R. Hen, J. Javitch, H. Mayberg, B. McEwen, M. J. Meaney, E. J. Nestler, Treatment resistant depression: A multi-scale, systems biology approach. *Neurosci. Biobehav. Rev.* **84**, 272–288 (2018).
4. A. Cipriani, T. A. Furukawa, G. Salanti, A. Chaimani, L. Z. Atkinson, Y. Ogawa, S. Leucht, H. G. Ruhe, E. H. Turner, J. P. T. Higgins, M. Egger, N. Takeshima, Y. Hayasaka, H. Imai, K. Shinohara, A. Tajika, J. P. A. Ioannidis, J. R. Geddes, Comparative efficacy and acceptability of 21 antidepressant drugs for the acute treatment of adults with major depressive disorder: A systematic review and network meta-analysis. *Lancet* **391**, 1357–1366 (2018).
5. A. J. Ferrari, F. J. Charlson, R. E. Norman, S. B. Patten, G. Freedman, C. J. L. Murray, T. Vos, H. A. Whiteford, Burden of depressive disorders by country, sex, age, and year: Findings from the global burden of disease study 2010. *PLOS Med.* **10**, e1001547 (2013).

6. J. J. Sramek, M. F. Murphy, N. R. Cutler, Sex differences in the psychopharmacological treatment of depression. *Dialogues Clin. Neurosci.* **18**, 447–457 (2016).
7. D. A. Bangasser, R. J. Valentino, Sex differences in stress-related psychiatric disorders: neurobiological perspectives. *Front. Neuroendocrinol.* **35**, 303–319 (2014).
8. T. L. Bale, C. N. Epperson, Sex differences and stress across the lifespan. *Nat. Neurosci.* **18**, 1413–1420 (2015).
9. M. B. Solomon, J. P. Herman, Sex differences in psychopathology: Of gonads, adrenals and mental illness. *Physiol. Behav.* **97**, 250–258 (2009).
10. O. Issler, E. J. Nestler, The molecular basis for sex differences in depression susceptibility. *Curr. Opin. Behav. Sci.* **23**, 1–6 (2018).
11. A. Torres-Berrio, O. Issler, E. M. Parise, E. J. Nestler, Unraveling the epigenetic landscape of depression: Focus on early life stress. *Dialogues Clin. Neurosci.* **21**, 341–357 (2019).
12. I. Ulitsky, Evolution to the rescue: Using comparative genomics to understand long non-coding RNAs. *Nat. Rev. Genet.* **17**, 601–614 (2016).
13. M. K. Iyer, Y. S. Niknafs, R. Malik, U. Singhal, A. Sahu, Y. Hosono, T. R. Barrette, J. R. Prensner, J. R. Evans, S. Zhao, A. Poliakov, X. Cao, S. M. Dhanasekaran, Y.-M. Wu, D. R. Robinson, D. G. Beer, F. Y. Feng, H. K. Iyer, A. M. Chinnaiyan, The landscape of long noncoding RNAs in the human transcriptome. *Nat. Genet.* **47**, 199–208 (2015).
14. J. D. Ransohoff, Y. Wei, P. A. Khavari, The functions and unique features of long intergenic non-coding RNA. *Nat. Rev. Mol. Cell Biol.* **19**, 143–157 (2018).
15. J. L. Rinn, H. Y. Chang, Long noncoding RNAs: Molecular modalities to organismal functions. *Annu. Rev. Biochem.* **89**, 283–308 (2020).
16. J. J. Quinn, H. Y. Chang, Unique features of long non-coding RNA biogenesis and function. *Nat. Rev. Genet.* **17**, 47–62 (2016).
17. O. Issler, Y. Y. van der Zee, A. Ramakrishnan, P. Wang, C. Tan, Y.-H. E. Loh, I. Purushothaman, D. M. Walker, Z. S. Lorsch, P. J. Hamilton, C. J. Peña, E. Flaherty, B. J. Hartley, A. Torres-Berrio, E. M. Parise, H. Kronman, J. E. Duffy, M. S. Estill, E. S. Calipari, B. Labonté, R. L. Neve, C. A. Tamminga, K. J. Brennand, Y. Dong, L. Shen, E. J. Nestler, Sex-specific role for the long non-coding RNA LINC00473 in depression. *Neuron* **106**, 912–926.e5 (2020).
18. Y. Zhou, P.-E. Lutz, Y. C. Wang, J. Ragoussis, G. Turecki, Global long non-coding RNA expression in the rostral anterior cingulate cortex of depressed suicides. *Transl. Psychiatry* **8**, 224 (2018).
19. Q. Wang, B. Roy, Y. Dwivedi, Co-expression network modeling identifies key long non-coding RNA and mRNA modules in altering molecular phenotype to develop stress-induced depression in rats. *Transl. Psychiatry* **9**, 125 (2019).
20. C. Li, F. Cao, S. Li, S. Huang, W. Li, N. Abumaria, Profiling and co-expression network analysis of learned helplessness regulated mRNAs and lncRNAs in the mouse hippocampus. *Front. Mol. Neurosci.* **10**, 454 (2018).
21. M. J. Girenti, J. Wang, D. Ji, D. A. Cruz; Traumatic Stress Brain Research Group, M. B. Stein, J. Gelernter, K. A. Young, B. R. Huber, D. E. Williamson, M. J. Friedman, J. H. Krystal, H. Zhao, R. S. Duman, Transcriptomic organization of the human brain in post-traumatic stress disorder. *Nat. Neurosci.* **24**, 24–33 (2021).
22. W. J. Kent, C. W. Sugnet, T. S. Furey, K. M. Roskin, T. H. Pringle, A. M. Zahler, D. Haussler, The human genome browser at UCSC. *Genome Res.* **12**, 996–1006 (2002).
23. GTEx Consortium, The genotype-tissue expression (GTEx) project. *Nat. Genet.* **45**, 580–585 (2013).
24. Y. Zhang, S. A. Sloan, L. E. Clarke, C. Caneda, C. A. Plaza, P. D. Blumenthal, H. Vogel, G. K. Steinberg, M. S. B. Edwards, G. Li, J. A. Duncan III, S. H. Cheshier, L. M. Shuer, E. F. Chang, G. A. Grant, M. G. H. Gephart, B. A. Barres, Purification and characterization of progenitor and mature human astrocytes reveals transcriptional and functional differences with mouse. *Neuron* **89**, 37–53 (2016).
25. R. L. Neve, K. A. Neve, E. J. Nestler, W. A. Carlezon Jr., Use of herpes virus amplicon vectors to study brain disorders. *Biotechniques* **39**, 381–391 (2005).
26. G. E. Hodes, M. L. Pfau, I. Purushothaman, H. F. Ahn, S. A. Golden, D. J. Christoffel, J. Magida, A. Brancato, A. Takahashi, M. E. Flanigan, C. Menard, H. Aleyasin, J. W. Koo, Z. S. Lorsch, J. Feng, M. Heshmati, M. Wang, G. Turecki, R. Neve, B. Zhang, L. Shen, E. J. Nestler, S. J. Russo, Sex differences in nucleus accumbens transcriptome profiles associated with susceptibility versus resilience to subchronic variable stress. *J. Neurosci.* **35**, 16362–16376 (2015).
27. N. Edgar, E. Sibille, A putative functional role for oligodendrocytes in mood regulation. *Transl. Psychiatry* **2**, e109 (2012).
28. E. Antontseva, N. Bondar, V. Reshetnikov, T. Merkulova, The effects of chronic stress on brain myelination in humans and in various rodent models. *Neuroscience* **441**, 226–238 (2020).
29. B. Labonté, O. Engmann, I. Purushothaman, C. Menard, J. Wang, C. Tan, J. R. Scarpa, G. Moy, Y.-H. E. Loh, M. Cahill, Z. S. Lorsch, P. J. Hamilton, E. S. Calipari, G. E. Hodes, O. Issler, H. Kronman, M. Pfau, A. L. J. Obradovic, Y. Dong, R. L. Neve, S. Russo, A. Kazarskis, C. Tamminga, N. Mechawar, G. Turecki, B. Zhang, L. Shen, E. J. Nestler, Sex-specific transcriptional signatures in human depression. *Nat. Med.* **23**, 1102–1111 (2017).
30. K. M. Cahill, Z. Huo, G. C. Tseng, R. W. Logan, M. L. Seney, Improved identification of concordant and discordant gene expression signatures using an updated rank-rank hypergeometric overlap approach. *Sci. Rep.* **8**, 9588 (2018).
31. D. A. Bangasser, A. Cuarenta, Sex differences in anxiety and depression: circuits and mechanisms. *Nat. Rev. Neurosci.* **22**, 674–684 (2021).
32. M. L. Seney, Z. Huo, K. Cahill, L. French, R. Puralewski, J. Zhang, R. W. Logan, G. Tseng, D. A. Lewis, E. Sibille, Opposite molecular signatures of depression in men and women. *Biol. Psychiatry* **84**, 18–27 (2018).
33. D. M. Walker, X. Zhou, A. M. Cunningham, A. P. Lipschultz, A. Ramakrishnan, H. M. Cates, R. C. Bagot, L. Shen, B. Zhang, E. J. Nestler, Sex-specific transcriptional changes in response to adolescent social stress in the brain's reward circuitry. *Biol. Psychiatry* **91**, 118–128 (2021).
34. T. Melia, P. Hao, F. Yilmaz, D. J. Waxman, Hepatic long intergenic noncoding RNAs: High promoter conservation and dynamic, sex-dependent transcriptional regulation by growth hormone. *Mol. Cell Biol.* **36**, 50–69 (2016).
35. T. Melia, D. J. Waxman, Sex-biased lncRNAs inversely correlate with sex-opposite gene coexpression networks in diversity outbred mouse liver. *Endocrinology* **160**, 989–1007 (2019).
36. W. Yuan, S. Jiang, D. Sun, Z. Wu, C. Wei, C. Dai, L. Jiang, S. Peng, Transcriptome profiling analysis of sex-based differentially expressed mRNAs and lncRNAs in the brains of mature zebrafish (*Danio rerio*). *BMC Genomics* **20**, 830 (2019).
37. J. B. Brown, N. Boley, R. Eisman, G. E. May, M. H. Stoiber, M. O. Duff, B. W. Booth, J. Wen, S. Park, A. M. Suzuki, K. H. Wan, C. Yu, D. Zhang, J. W. Carlson, L. Cherbas, B. D. Eads, D. Miller, K. Mockaitis, J. Roberts, C. A. Davis, E. Frise, A. S. Hammonds, S. Olson, S. Shenker, D. Sturgill, A. A. Samsonova, R. Weiszmann, G. Robinson, J. Hernandez, J. Andrews, P. J. Bickel, P. Carninci, P. Cherbas, T. R. Gingeras, R. A. Hoskins, T. C. Kaufman, E. C. Lai, B. Oliver, N. Perrimon, B. R. Graveley, S. E. Celnikier, Diversity and dynamics of the *Drosophila* transcriptome. *Nature* **512**, 393–399 (2014).
38. M. Keshavarz, D. Tautz, The imprinted lncRNA *Peg13* regulates sexual preference and the sex-specific brain transcriptome in mice. *Proc. Natl. Acad. Sci. U.S.A.* **118**, e2022172118 (2021).
39. Z. Lu, A. C. Carter, H. Y. Chang, Mechanistic insights in X-chromosome inactivation. *Philos. Trans. R. Soc. Lond. B Biol. Sci.* **372**, 20160356 (2017).
40. S. Gayen, E. Maclary, M. Hinten, S. Kalantry, Sex-specific silencing of X-linked genes by Xist RNA. *Proc. Natl. Acad. Sci. U.S.A.* **113**, E309–E318 (2016).
41. S. Darmanis, S. A. Sloan, Y. Zhang, M. Enge, C. Caneda, L. M. Shuer, M. G. Hayden Gephart, B. A. Barres, S. R. Quake, A survey of human brain transcriptome diversity at the single cell level. *Proc. Natl. Acad. Sci. U.S.A.* **112**, 7285–7290 (2015).
42. O. Rivero, M. M. Selten, S. Sich, S. Popp, L. Bacmeister, E. Amendola, M. Negwer, D. Schubert, F. Proft, D. Kiser, A. G. Schmitt, C. Gross, S. M. Kolk, T. Strelakova, D. van den Hove, T. J. Resink, N. Nadif Kasri, K. P. Lesch, Cadherin-13, a risk gene for ADHD and comorbid disorders, impacts GABAergic function in hippocampus and cognition. *Transl. Psychiatry* **5**, e655 (2015).
43. O. Rivero, S. Sich, S. Popp, A. Schmitt, B. Franke, K.-P. Lesch, Impact of the ADHD-susceptibility gene *CDH13* on development and function of brain networks. *Eur. Neuropsychopharmacol.* **23**, 492–507 (2013).
44. J. Treutlein, S. Cichon, M. Ridinger, N. Wodarz, M. Soyka, P. Zill, W. Maier, R. Moessner, W. Gaebel, N. Dahmen, C. Fehr, N. Scherbaum, M. Steffens, K. U. Ludwig, J. Frank, H. E. Wichmann, S. Schreiber, N. Dragano, W. H. Sommer, F. Leonardi-Essmann, A. Lourdasamy, P. Gebicke-Haerter, T. F. Wienker, P. F. Sullivan, M. M. Nöthen, F. Kiefer, R. Spanagel, K. Mann, M. Rietschel, Genome-wide association study of alcohol dependence. *Arch. Gen. Psychiatry* **66**, 773–784 (2009).
45. M. Sokolowski, J. Wasserman, D. Wasserman, Polygenic associations of neurodevelopmental genes in suicide attempt. *Mol. Psychiatry* **21**, 1381–1390 (2016).
46. T. S. Wingo, Y. Liu, E. S. Gerasimov, J. Gockley, B. A. Logsdon, D. M. Duong, E. B. Dammer, A. Lori, P. J. Kim, K. J. Ressler, T. G. Beach, E. M. Reiman, M. P. Epstein, P. L. de Jager, J. J. Lah, D. A. Bennett, N. T. Seyfried, A. I. Levey, A. P. Wingo, Brain proteome-wide association study implicates novel proteins in depression pathogenesis. *Nat. Neurosci.* **24**, 810–817 (2021).
47. N. Hoshina, E. M. Johnson-Venkatesh, M. Hoshina, H. Umemori, Female-specific synaptic dysfunction and cognitive impairment in a mouse model of *PCDH19* disorder. *Science* **372**, eaaz3893 (2021).
48. R. C. Bagot, H. M. Cates, I. Purushothaman, Z. S. Lorsch, D. M. Walker, J. Wang, X. Huang, O. M. Schlüter, I. Maze, C. J. Peña, E. A. Heller, O. Issler, M. Wang, W.-M. Song, J. L. Stein, X. Liu, M. A. Doyle, K. N. Scobie, H. S. Sun, R. L. Neve, D. Geschwind, Y. Dong, L. Shen, B. Zhang, E. J. Nestler, Circuit-wide transcriptional profiling reveals brain region-specific gene networks regulating depression susceptibility. *Neuron* **90**, 969–983 (2016).

49. H. J. Kang, B. Voleti, T. Hajszan, G. Rajkowska, C. A. Stockmeier, P. Licznanski, A. Lepak, M. S. Majik, L. S. Jeong, M. Banasr, H. Son, R. S. Duman, Decreased expression of synapse-related genes and loss of synapses in major depressive disorder. *Nat. Med.* **18**, 1413–1417 (2012).
50. A. M. Feyissa, A. Chandran, C. A. Stockmeier, B. Karolewicz, Reduced levels of NR2A and NR2B subunits of NMDA receptor and PSD-95 in the prefrontal cortex in major depression. *Prog. Neuropsychopharmacol. Biol. Psychiatry* **33**, 70–75 (2009).
51. N. Li, R. J. Liu, J. M. Dwyer, M. Banasr, B. Lee, H. Son, X. Y. Li, G. Aghajanian, R. S. Duman, Glutamate N-methyl-D-aspartate receptor antagonists rapidly reverse behavioral and synaptic deficits caused by chronic stress exposure. *Biol. Psychiatry* **69**, 754–761 (2011).
52. J. P. Lopez, E. Brivio, A. Santambrogio, C. de Donno, A. Kos, M. Peters, N. Rost, D. Czamara, T. M. Brückl, S. Roeh, M. L. Pöhlmann, C. Engelhardt, A. Ressler, R. Stoffel, A. Tontsch, J. M. Villamizar, M. Reincke, A. Riestler, S. Sberia, M. Fassnacht, H. S. Mayberg, W. E. Craighead, B. W. Dunlop, C. B. Nemeroff, M. V. Schmidt, E. B. Binder, F. J. Theis, F. Beuschlein, C. L. Andoniadou, A. Chen, Single-cell molecular profiling of all three components of the HPA axis reveals adrenal ABCB1 as a regulator of stress adaptation. *Sci. Adv.* **7**, eabe4497 (2021).
53. T. P. Bittar, M. C. Pelaez, J. C. Hernandez Silva, F. Quessy, A.-A. Lavigne, D. Morency, L.-J. Blanchette, E. Arseneault, Y. Cherasse, J. Seigneur, I. Timofeev, C. F. Sephton, C. D. Proulx, B. Labonté, Chronic stress induces sex-specific functional and morphological alterations in corticoaccumbal and corticocortical pathways. *Biol. Psychiatry* **90**, 194–205 (2021).
54. M. W. Tham, P. S. Woon, M. Y. Sum, T.-S. Lee, K. Sim, White matter abnormalities in major depression: Evidence from post-mortem, neuroimaging and genetic studies. *J. Affect. Disord.* **132**, 26–36 (2011).
55. E. Boda, Myelin and oligodendrocyte lineage cell dysfunctions: New players in the etiology and treatment of depression and stress-related disorders. *Eur. J. Neurosci.* **53**, 281–297 (2021).
56. W. T. Regenold, P. Phatak, C. M. Marano, L. Gearhart, C. H. Viens, K. C. Hisley, Myelin staining of deep white matter in the dorsolateral prefrontal cortex in schizophrenia, bipolar disorder, and unipolar major depression. *Psychiatry Res.* **151**, 179–188 (2007).
57. Y. Hayashi, N. Nihonmatsu-Kikuchi, X. Yu, K. Ishimoto, S. I. Hisanaga, Y. Tatebayashi, A novel, rapid, quantitative cell-counting method reveals oligodendroglial reduction in the frontopolar cortex in major depressive disorder. *Mol. Psychiatry* **16**, 1155–1158 (2011).
58. T. A. Klempan, A. Sequeira, L. Canetti, A. Lalovic, C. Ernst, J. French-Mullen, G. Turecki, Altered expression of genes involved in ATP biosynthesis and GABAergic neurotransmission in the ventral prefrontal cortex of suicides with and without major depression. *Mol. Psychiatry* **14**, 175–189 (2009).
59. S. Kim, M. J. Webster, Correlation analysis between genome-wide expression profiles and cytoarchitectural abnormalities in the prefrontal cortex of psychiatric disorders. *Mol. Psychiatry* **15**, 326–336 (2010).
60. C. Nagy, M. Maitra, A. Tanti, M. Suderman, J.-F. Thérout, M. A. Davoli, K. Perlman, V. Yerko, Y. C. Wang, S. J. Tripathy, P. Pavlidis, N. Mechawar, J. Ragoussis, G. Turecki, Single-nucleus transcriptomics of the prefrontal cortex in major depressive disorder implicates oligodendrocyte precursor cells and excitatory neurons. *Nat. Neurosci.* **23**, 771–781 (2020).
61. G. Rajkowska, G. Mahajan, D. Maciag, M. Sathyanesan, A. H. Iyo, M. Moulana, P. B. Kyle, W. L. Woolverton, J. J. Miguel-Hidalgo, C. A. Stockmeier, S. S. Newton, Oligodendrocyte morphometry and expression of myelin-Related mRNA in ventral prefrontal white matter in major depressive disorder. *J. Psychiatr. Res.* **65**, 53–62 (2015).
62. M. Banasr, G. W. Valentine, X. Y. Li, S. L. Gourley, J. R. Taylor, R. S. Duman, Chronic unpredictable stress decreases cell proliferation in the cerebral cortex of the adult rat. *Biol. Psychiatry* **62**, 496–504 (2007).
63. M. Wennström, J. Hellsten, J. Ekstrand, H. Lindgren, A. Tingstrom, Corticosterone-induced inhibition of gliogenesis in rat hippocampus is counteracted by electroconvulsive seizures. *Biol. Psychiatry* **59**, 178–186 (2006).
64. B. Czéh, J. I. H. Müller-Keuker, R. Rygula, N. Abumaria, C. Hiemke, E. Domenici, E. Fuchs, Chronic social stress inhibits cell proliferation in the adult medial prefrontal cortex: Hemispheric asymmetry and reversal by fluoxetine treatment. *Neuropsychopharmacology* **32**, 1490–1503 (2007).
65. M. L. Lehmann, T. K. Weigel, A. G. Elkhoulou, M. Herkenham, Chronic social defeat reduces myelination in the mouse medial prefrontal cortex. *Sci. Rep.* **7**, 46548 (2017).
66. V. Bonnefil, K. Dietz, M. Amatruda, M. Wentling, A. V. Aubry, J. L. Dupree, G. Temple, H.-J. Park, N. S. Burghardt, P. Casaccia, J. Liu, Region-specific myelin differences define behavioral consequences of chronic social defeat stress in mice. *eLife* **8**, e40855 (2019).
67. J. Liu, K. Dietz, J. M. DeLoyht, X. Pedre, D. Kelkar, J. Kaur, V. Vialou, M. K. Lobo, D. M. Dietz, E. J. Nestler, J. Dupree, P. Casaccia, Impaired adult myelination in the prefrontal cortex of socially isolated mice. *Nat. Neurosci.* **15**, 1621–1623 (2012).
68. J. Liu, J. L. Dupree, M. Gacias, R. Frawley, T. Sikder, P. Naik, P. Casaccia, Clemastine enhances myelination in the prefrontal cortex and rescues behavioral changes in socially isolated mice. *J. Neurosci.* **36**, 957–962 (2016).
69. R. D. Fields, A new mechanism of nervous system plasticity: Activity-dependent myelination. *Nat. Rev. Neurosci.* **16**, 756–767 (2015).
70. S. E. Pease-Raisi, J. R. Chan, Building a (w)rapport between neurons and oligodendroglia: Reciprocal interactions underlying adaptive myelination. *Neuron* **109**, 1258–1273 (2021).
71. O. de Faria, H. Pivonkova, B. Varga, S. Timmler, K. A. Evans, R. T. Kárádóttir, Periods of synchronized myelin changes shape brain function and plasticity. *Nat. Neurosci.* **24**, 1508–1521 (2021).
72. T. T. Le, J. Savitz, H. Suzuki, M. Misaki, T. K. Teague, B. C. White, J. H. Marino, G. Wiley, P. M. Gaffney, W. C. Drevets, B. A. Mc Kinney, J. Bodurka, Identification and replication of RNA-seq gene network modules associated with depression severity. *Transl. Psychiatry* **8**, 180 (2018).
73. Y. Zhu, E. Strachan, E. Fowler, T. Bacus, P. Roy-Byrne, J. Zhao, Genome-wide profiling of DNA methylome and transcriptome in peripheral blood monocytes for major depression: A monozygotic discordant twin study. *Transl. Psychiatry* **9**, 215 (2019).
74. S. Mostafavi, A. Battle, X. Zhu, J. B. Potash, M. M. Weissman, J. Shi, K. Beckman, C. Haudenschild, C. McCormick, R. Mei, M. J. Gameroff, H. Gindes, P. Adams, F. S. Goes, F. M. Mondimore, D. F. MacKinnon, L. Notes, B. Schweizer, D. Furman, S. B. Montgomery, A. E. Urban, D. Koller, D. F. Levinson, Type I interferon signaling genes in recurrent major depression: Increased expression detected by whole-blood RNA sequencing. *Mol. Psychiatry* **19**, 1267–1274 (2014).
75. K. N. Wright, M. Kabbaj, Sex differences in sub-anesthetic ketamine's antidepressant effects and abuse liability. *Curr. Opin. Behav. Sci.* **23**, 36–41 (2018).
76. D. M. Gerhard, R. S. Duman, Rapid-acting antidepressants: Mechanistic insights and future directions. *Curr. Behav. Neurosci. Rep.* **5**, 36–47 (2018).
77. B. Romeo, W. Choucha, P. Fossati, J.-Y. Rotge, Meta-analysis of short- and mid-term efficacy of ketamine in unipolar and bipolar depression. *Psychiatry Res.* **230**, 682–688 (2015).
78. C. M. Coyle, K. R. Laws, The use of ketamine as an antidepressant: A systematic review and meta-analysis. *Hum. Psychopharmacol.* **30**, 152–163 (2015).
79. G. Monaco, B. Lee, W. Xu, S. Mustafah, Y. Y. Hwang, C. Carré, N. Burdin, L. Visan, M. Ceccarelli, M. Poidinger, A. Zippelius, J. P. de Magalhães, A. Larbi, RNA-seq signatures normalized by mRNA abundance allow absolute deconvolution of human immune cell types. *Cell Rep.* **26**, 1627–1640.e7 (2019).
80. F. Cathomas, J. W. Murrrough, E. J. Nestler, M.-H. Han, S. J. Russo, Neurobiology of resilience: Interface between mind and body. *Biol. Psychiatry* **86**, 410–420 (2019).
81. X. Ruan, P. Li, Y. Chen, Y. Shi, M. Pirooznia, F. Seifuddin, H. Suemizu, Y. Ohnishi, N. Yoneda, M. Nishiwaki, J. Shepherdson, A. Suresh, K. Singh, Y. Ma, C.-F. Jiang, H. Cao, In vivo functional analysis of non-conserved human lncRNAs associated with cardiometabolic traits. *Nat. Commun.* **11**, 45 (2020).
82. E. R. E. Schmidt, H. T. Zhao, J. M. Park, M. Dipoppa, M. M. Monsalve-Mercado, J. B. Dahan, C. C. Rodgers, A. Lejeune, E. M. C. Hillman, K. D. Miller, R. M. Bruno, F. Polleux, A human-specific modifier of cortical connectivity and circuit function. *Nature* **599**, 640–644 (2021).
83. Z. S. Lorsch, Y.-H. E. Loh, I. Purushothaman, D. M. Walker, E. M. Parise, M. Salery, M. E. Cahill, G. E. Hodes, M. L. Pfau, H. Kronman, P. J. Hamilton, O. Issler, B. Labonté, A. E. Symonds, M. Zucker, T. Y. Zhang, M. J. Meaney, S. J. Russo, L. Shen, R. C. Bagot, E. J. Nestler, Estrogen receptor  $\alpha$  drives pro-resilient transcription in mouse models of depression. *Nat. Commun.* **9**, 1116 (2018).
84. C. J. Peña, H. G. Kronman, D. M. Walker, H. M. Cates, R. C. Bagot, I. Purushothaman, O. Issler, Y.-H. E. Loh, T. Leong, D. D. Kiraly, E. Goodman, R. L. Neve, L. Shen, E. J. Nestler, Early life stress confers lifelong stress susceptibility in mice via ventral tegmental area OTX2. *Science* **356**, 1185–1188 (2017).
85. H. Sun, D. M. Domez-Werno, K. N. Scobie, N.-Y. Shao, C. Dias, J. Rabkin, J. W. Koo, E. Korb, R. C. Bagot, F. H. Ahn, M. E. Cahill, B. Labonté, E. Mouzon, E. A. Heller, H. Cates, S. A. Golden, K. Gleason, S. J. Russo, S. Andrews, R. Neve, P. J. Kennedy, I. Maze, D. M. Dietz, C. D. Allis, G. Turecki, P. Varga-Weisz, C. Tamminga, L. Shen, E. J. Nestler, ACF chromatin-remodeling complex mediates stress-induced depressive-like behavior. *Nat. Med.* **21**, 1146–1153 (2015).
86. E. M. Anderson, H. Sun, D. Guzman, M. Taniguchi, C. W. Cowan, I. Maze, E. J. Nestler, D. W. Self, Knockdown of the histone di-methyltransferase G9a in nucleus accumbens shell decreases cocaine self-administration, stress-induced reinstatement, and anxiety. *Neuropsychopharmacology* **44**, 1370–1376 (2019).
87. C. J. Browne, A. R. Abela, D. Chu, Z. Li, X. Ji, E. K. Lambe, P. J. Fletcher, Dorsal raphe serotonin neurons inhibit operant responding for reward via inputs to the ventral tegmental area but not the nucleus accumbens: Evidence from studies combining optogenetic stimulation and serotonin reuptake inhibition. *Neuropsychopharmacology* **44**, 793–804 (2019).

88. G. von Jonquieres, D. Fröhlich, C. B. Klugmann, X. Wen, A. E. Harasta, R. Ramkumar, Z. H. T. Spencer, G. D. Housley, M. Klugmann, Recombinant human myelin-associated glycoprotein promoter drives selective AAV-mediated transgene expression in oligodendrocytes. *Front Mol. Neurosci.* **9**, 13 (2016).
89. D. I. Kim, J. M. Paggi, C. Park, C. Bennett, S. L. Salzberg, Graph-based genome alignment and genotyping with HISAT2 and HISAT-genotype. *Nat. Biotechnol.* **37**, 907–915 (2019).
90. A. Andrews, FastQC: A quality control tool for high throughput sequence data, (2010); <https://www.bioinformatics.babraham.ac.uk/projects/fastqc/>.
91. M. I. Love, W. Huber, S. Anders, Moderated estimation of fold change and dispersion for RNA-seq data with DESeq2. *Genome Biol.* **15**, 550 (2014).
92. M. V. Kuleshov, M. R. Jones, A. D. Rouillard, N. F. Fernandez, Q. Duan, Z. Wang, S. Koplev, S. L. Jenkins, K. M. Jagodnik, A. Lachmann, M. G. McDermott, C. D. Monteiro, G. W. Gundersen, A. Ma'ayan, Enrichr: A comprehensive gene set enrichment analysis web server 2016 update. *Nucleic Acids Res.* **44**, W90–W97 (2016).
93. F. Koopmans, P. van Nierop, M. Andres-Alonso, A. Byrnes, T. Cijssouw, M. P. Coba, L. N. Cornelisse, R. J. Farrell, H. L. Goldschmidt, D. P. Howrigan, N. K. Hussain, C. Imig, A. P. H. de Jong, H. Jung, M. Kohansalnodehi, B. Kramarz, N. Lipstein, R. C. Lovering, H. M. Gillavry, V. Mariano, H. Mi, M. Ninov, D. Osumi-Sutherland, R. Pielot, K.-H. Smalla, H. Tang, K. Tashman, R. F. G. Toonen, C. Verpelli, R. Reig-Viader, K. Watanabe, J. van Weering, T. Achsel, G. Ashrafi, N. Asi, T. C. Brown, P. De Camilli, M. Feuermann, R. E. Foulger, P. Gaudet, A. Joglekar, A. Kanellopoulos, R. Malenka, R. A. Nicoll, C. Pulido, J. de Juan-Sanz, M. Sheng, T. C. Südhof, H. U. Tilgner, C. Bagni, À. Bayés, T. Biederer, N. Brose, J. J. E. Chua, D. C. Dieterich, E. D. Gundelfinger, C. Hoogenraad, R. L. Huganir, R. Jahn, P. S. Kaeser, E. Kim, M. R. Kreutz, P. S. McPherson, B. M. Neale, V. O' Connor, D. Posthuma, T. A. Ryan, C. Sala, G. Feng, S. E. Hyman, P. D. Thomas, A. B. Smit, M. Verhage, SynGO: An evidence-based, expert-curated knowledge base for the synapse. *Neuron* **103**, 217–234.e4 (2019).
94. A. T. McKenzie, M. Wang, M. E. Hauberg, J. F. Fullard, A. Kozlenkov, A. Keenan, Y. L. Hurd, S. Dracheva, P. Casaccia, P. Rousos, B. Zhang, Brain cell type specific gene expression and co-expression network architectures. *Sci. Rep.* **8**, 8868 (2018).
95. Y. van der Zee, L. M. T. Eijssen, P. Mews, A. Ramakrishnan, K. Alvarez, C. K. Lardner, H. M. Cates, D. M. Walker, A. Torres-Berrio, C. J. Browne, A. Cunningham, F. Cathomas, H. Kronman, E. M. Parise, L. de Nijs, L. Shen, J. W. Murrrough, B. P. F. Rutten, E. J. Nestler, O. Issler, Blood miR-144-3p: A novel diagnostic and therapeutic tool for depression. *Mol. Psychiatry* 10.1038/s41380-022-01712-6, (2022).
96. F. Cathomas, L. Bevilacqua, A. Ramakrishnan, H. Kronman, S. Costi, M. Schneider, K. L. Chan, L. Li, E. J. Nestler, L. Shen, D. S. Charney, S. J. Russo, J. W. Murrrough, Whole blood transcriptional signatures associated with rapid antidepressant response to ketamine in patients with treatment resistant depression. *Transl. Psychiatry.* **12**, 12 (2022).

**Acknowledgments:** We thank G. von Jonquieres and M. Klugmann from UNSW Sydney, Australia, for sharing the oligodendrocyte specific (MAG promoter) plasmids, R. Neve for the production of the HSV, J. Gregory for illustrations and F. Cathomas for help with the blood samples. **Funding:** This work was funded by the National Institute of Mental Health (R01MH051399) and Hope for Depression Research Foundation (HDRF). **Author contributions:** Conceptualization: O.I. and E.J.N. Formal analysis: O.I., A.R., L.S., C.T., W.L., S.X., A.K.Z., Y.D., and J.L.D. Methodology: O.I. Software: A.R. and L.S. Resources: J.W.M., C.A.T., B.L., and M.J.G. Investigation: O.I., Y.Y.v.d.Z., C.T., W.L., S.X., A.K.Z., M.S., C.J.B., D.M.W., A.T.-B., R.F., and J.E.D. Visualization: O.I. and Y.Y.v.d.Z. Funding acquisition: E.J.N. Supervision: O.I. and E.J.N. Writing (original draft): O.I. Writing (review and editing): E.J.N., C.J.B., and L.S. **Competing interests:** The Icahn School of Medicine has filed and was awarded patents (U.S. patent no. 9,592,207; no. 8,785,500) and has entered into a licensing agreement and will receive payments related to the use of ketamine or esketamine for the treatment of depression. None of the authors of this manuscript are named on these patents and will receive no payments. The authors declare that they have no other competing interests. **Data and materials availability:** Raw RNA-seq data were deposited in GEO (GSE188930). All data needed to evaluate the conclusions in the paper are present in the paper and/or the Supplementary Materials.

Submitted 3 January 2022  
Accepted 12 October 2022  
Published 30 November 2022  
10.1126/sciadv.abn9494